

AD-A136 956

EVALUATION OF FATIGUE-CREEP CRACK GROWTH IN AN ENGINE  
ALLOY(U) AIR FORCE INST OF TECH WRIGHT-PATTERSON AFB OH  
SCHOOL OF ENGINEERING J R CHRISTOFF DEC 83

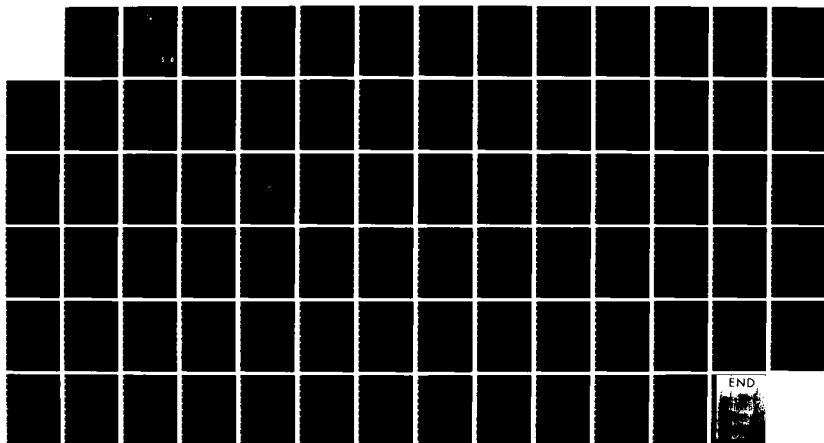
1/1

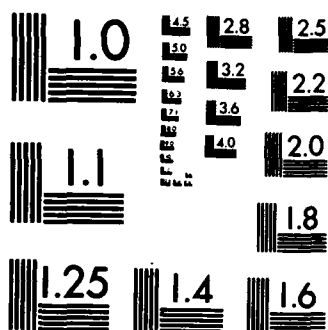
UNCLASSIFIED

AFIT/GA/AA/83D-2

F/G 11/6

NL





MICROCOPY RESOLUTION TEST CHART  
NATIONAL BUREAU OF STANDARDS-1963-A

AD A136956



EVALUATION OF FATIGUE-CREEP  
CRACK GROWTH IN AN ENGINE  
ALLOY

THESIS

Jeffery R. Christoff  
Second Lieutenant, USAF

AFIT/GA/AA/83D-2

DTIC FILE COPY

DEPARTMENT OF THE AIR FORCE  
AIR UNIVERSITY

**AIR FORCE INSTITUTE OF TECHNOLOGY**

DTIC  
ELECTE  
JAN 19 1984  
S D E

Wright-Patterson Air Force Base, Ohio

This document has been approved  
for public release and sale; its  
distribution is unlimited.

84 01 17 060

AFIT/GA/AA/83D-2

EVALUATION OF FATIGUE-CREEP  
CRACK GROWTH IN AN ENGINE  
ALLOY

THESIS

Jeffery R. Christoff  
Second Lieutenant, USAF

AFIT/GA/AA/83D-2

DTIC  
ELECTE  
S JAN 19 1984 D  
E

Approved for public release; distribution unlimited

## Abstract

→ This study investigates fatigue-creep interaction effects in alloys and evaluates the effectiveness of predictive models currently in use by the aircraft engine industry. The state-of-the-art crack growth rate prediction models are supplied by the General Electric Company (MSE) model, and the Pratt and Whitney Aircraft Group (SINH) model. They are used to predict crack growth rates under a range of conditions which involve fatigue-creep interactions.

Another aspect of this study involves the development of an empirical model to predict fatigue-creep crack growth based on creep crack growth rate data and knowledge of the loading wave-form. This study is primarily directed toward high temperature ( $\geq 1000$  F) fatigue-creep interaction at low test frequencies <sup>> or =</sup> and positive stress ratios.

The SINH model proves to be more accurate than the MSE model in predicting crack growth rates for the data analyzed. Both models predict linear relationships for the variation of crack growth rates ( $da/dN$ ) with the length of hold-time or the frequency rate on logarithmic coordinates. ← The MSE model is developed for AF115, whereas the SINH model has the ability to adapt to any high-strength material.

The predictive model, developed in this paper, compares well with experimental fatigue-creep crack growth rate data that are mostly in the time-dependent regime, that is, when

EVALUATION OF FATIGUE-CREEP  
CRACK GROWTH IN AN ENGINE ALLOY

THESIS

Presented to the Faculty of the School of Engineering  
of the Air Force Institute of Technology

Air University

In Partial Fulfillment of the  
Requirements of the Degree of  
Master of Science in Astronautical Engineering

Jeffery R. Christoff, B.S.  
Second Lieutenant, USAF

December 83

Approved for public release; distribution unlimited

### Acknowledgments

I wish to express my extreme gratitude to my thesis advisor Major George Haritos for his patience and expert judgment throughout this thesis.

I would like to thank the Air Force Materials Laboratory, in particular Dr. Ted Nicholas and Jim Larsen for the support necessary to conduct this analysis.

Special thanks is extended to Jim Laflen and David Utah of the General Electric Company at Evensdale, Ohio for their invaluable assistance with the program that was supplied for my research.

Jeffery R. Christoff

|                    |                                     |
|--------------------|-------------------------------------|
| Accession For      |                                     |
| NTIS GRA&I         | <input checked="" type="checkbox"/> |
| DTIC TAB           | <input type="checkbox"/>            |
| Unannounced        | <input type="checkbox"/>            |
| Justification      |                                     |
| By                 |                                     |
| Distribution/      |                                     |
| Availability Codes |                                     |
| Dist               | Avail and/or<br>Special             |
| A-1                |                                     |



## Table of Contents

|  | page |
|--|------|
| Acknowledgements . . . . .                         | iii  |
| Abstract . . . . .                                 | v    |
| I. Introduction . . . . .                          | 1    |
| II. Approach . . . . .                             | 5    |
| III. Numerical Analysis . . . . .                  | 14   |
| The Pratt and Whitney (SINH) Model . . . . .       | 14   |
| The General Electric (MSE) Model . . . . .         | 17   |
| Predictive Model . . . . .                         | 22   |
| IV. Results and Discussion . . . . .               | 29   |
| V. Conclusions and Recommendations . . . . .       | 47   |
| SINH . . . . .                                     | 47   |
| MSE . . . . .                                      | 49   |
| SINH-MSE Comparison . . . . .                      | 49   |
| Predictive Model . . . . .                         | 50   |
| Appendix A: Development of SINH Model . . . . .    | 52   |
| Appendix B: MSE Computer Code . . . . .            | 59   |
| Appendix C: AF115 Experimental Procedure . . . . . | 63   |
| Bibliography . . . . .                             | 69   |
| Vita . . . . .                                     | 71   |

hold-times are in excess of 5 seconds or the frequency is less than .02 cycles/second. This model correlates well with experimental data tested at these conditions.

# Evaluation of Fatigue-Creep Crack Growth in an Engine Alloy

## I. Introduction

Ever increasing performance requirements for U.S. Air Force turbine engines have placed stringent demands on material capability. A need to increase the ratio of engine thrust to weight has forced design stresses to higher levels, approaching the materials yield strength. At the same time engine operating temperatures have also continued to increase. In the hot section of the engine, turbine disks operate under severe thermal and mechanical loading. The variety of operating conditions within the engine dictate diverse material capability requirements. Thus, the disks materials must exhibit both strength at high temperature and creep resistance.

In the 1960's, the primary design limitations for turbine components were material strength and creep resistance. However, by 1975 low cycle fatigue (LCF) performance had become the life limiting factor for over 75% of the major structural components in advanced engines such as the F-100 which powers the Air Forces F-15 and F-16 aircraft (1:355). The present design philosophy is based entirely on the concepts of fatigue crack initiation (2,3). Any additional component life due to subcritical crack propagation following initiation is not considered.

According to the initiation philosophy, 1 out of 1000 of these components will have a measurable flaw, while the remaining components have not exhausted their initiation life. The difference between the design life of a disk and the mean life-time of all disks may be an order of magnitude or more. The present forced retirement policy requires the elimination of 999 statistically sound disks out of 1000. Although this design approach is extremely conservative, it is considered necessary for major structural components whose failure may have catastrophic results.

However, turbine engine components are becoming increasingly costly to replace; moreover, they are made of materials which are of limited domestic supply. Therefore, both from an economic and from a strategic viewpoint, it is desirable to fully utilize the available component life, provided it can be done without sacrificing safety. To accomplish this, an alternative approach to life management of engine components has been proposed. This new philosophy bases component life prediction upon both the initiation and stable growth of cracks in LCF limited components. This philosophy recommends tracking of individual engine components and that removal from service decisions be based on individual component capability rather than on a worst case analysis for the entire population of components.

The replacement of a safe life design policy by one of "fly to a safe crack" has been termed retirement for cause (RFC) (4;5). This approach is being considered for use in

military engines by the U.S. Air Force. RFC is based on statistical considerations that most disks have no detectable cracks when they reach their design life and would then have some useful life remaining. At present, each component is retired from service when it has reached its design life, whether or not any cracks are found. Under RFC, components would be kept in service and inspected at predetermined intervals for fatigue cracks. Components with no detectable cracks would be kept in service for another inspection interval. Conversely, if a crack were detected, then that part would be retired for cause. Fracture mechanics analysis would ensure that a crack smaller than the detectable size would not grow to a critical size in less time than the specified inspection interval multiplied by some factor of safety, e.g. 2 or 3. This procedure provides several opportunities to detect a crack before it reaches its critical length. It is obvious then that the reliability of both the inspection techniques and the crack growth predictions are vital aspects of RFC.

Three primary issues must be addressed for the successful implementation of an RFC approach to fleet management. The first one concerns the inspectability of cracks or flaws. A nondestructive evaluation (NDE) procedure which is both reliable and accurate must be available. The second one deals with the ability to predict the rate of growth of a crack under the loading and temperature conditions which will be encountered in the

design mission. The third one considers the economic aspects of the RFC concepts including inspection costs, replacement costs, and statistics of safety and reliability. In this paper, the predictions of crack growth behavior will be considered.

A typical loading spectrum for a turbine engine disk is composed of a mix of high and low stress fatigue cycles and various periods of sustained loading. Typical fatigue cycles generally have a frequency of 0.1Hz or slower, and are of the order of minutes. At high temperatures crack propagation produced by mission loading is quite complex, requiring the capability to predict the effects of fatigue and creep, and their interactions. It is the aim of this study to investigate these fatigue-creep interaction effects. This is done by implementing the state of the art crack growth rate prediction models currently used in industry. These models were developed by the General Electric Company (6) and the Pratt and Whitney Aircraft Group (7) to predict crack growth rate under a range of conditions which involve fatigue-creep interactions. Another aspect of this study involved the development of an empirical model to predict fatigue-creep crack growth based on creep crack growth data and knowledge of the loading wave-form. This effort is primarily directed toward high temperature ( $\geq 1000$  F) fatigue-creep interaction at low test frequencies and positive stress ratios, as this represents the main area of concern.

## II. Approach

The crack growth models used were those developed by the General Electric Company (6) and the Pratt and Whitney Aircraft Company (7). Both crack growth computer programs are empirical models based on the sigmoidal shape of the crack growth rate ( $da/dN$ ) versus stress intensity range ( $\Delta K$ ) curve. An example of such a graph is illustrated in Figure 1.

Both models attempt to predict the crack growth rate behavior in Regions I and III along with the usual straight line portion of Region II. In many materials, especially at high temperatures and stresses, the linear portion of Figure 1 is very narrow or nonexistent (8:226). Therefore, accurate and reliable predictions of crack growth rate behavior in Regions I and III are required by these crack growth models. The model developed by the Pratt and Whitney Company uses a hyperbolic sine equation fitted to a set of experimental data by the method of least squares (SINH model). This model has the capability of predicting crack growth for various temperatures, stress ratios, frequencies, and hold-times of various duration. The form of the hyperbolic sine equation used in this model is given in Eq (1)

$$\text{Log } (da/dN) = C_1 \sinh (C_2(\log(\Delta K) + C_3)) + C_4 \quad (1)$$

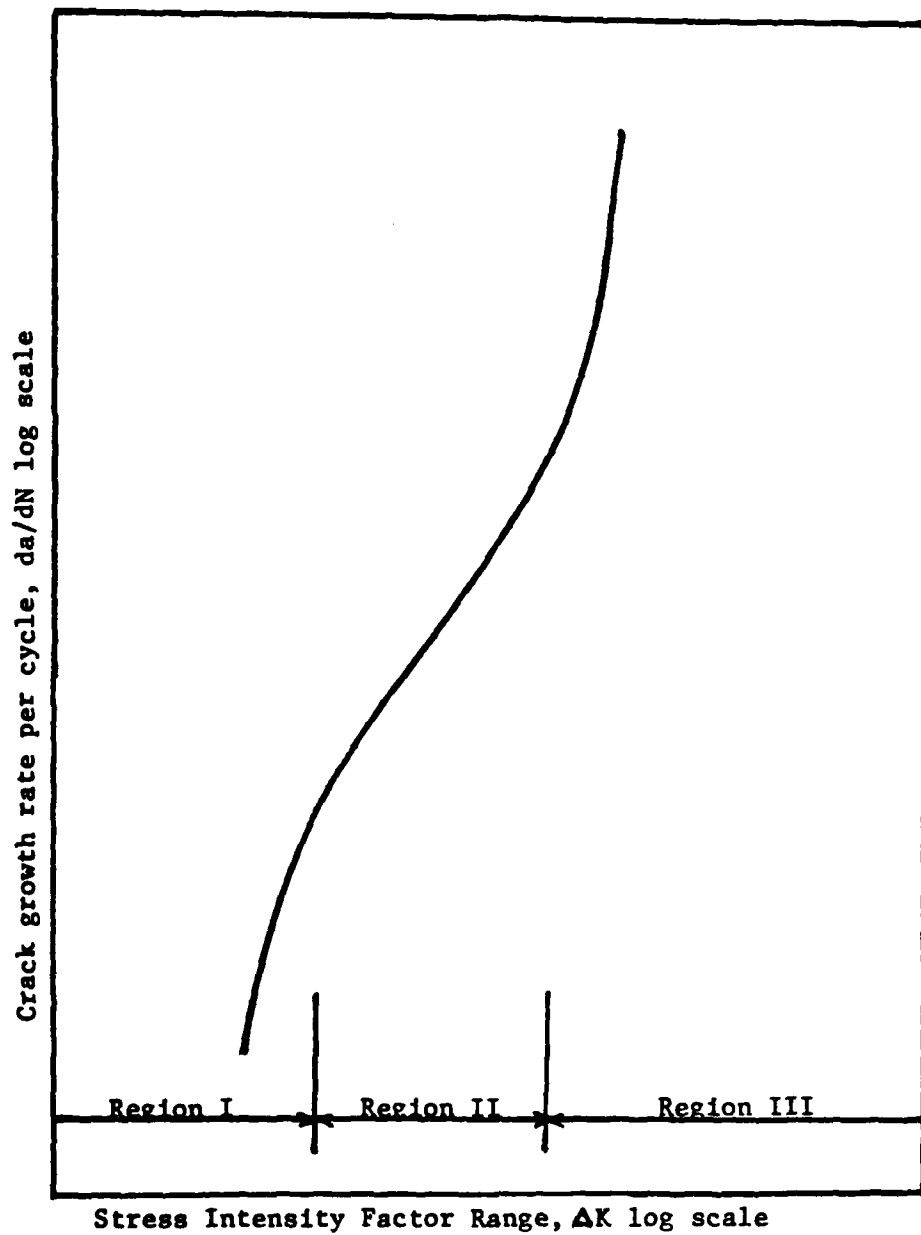


Figure 1. Schematic representation of fatigue crack growth rate.

where

$C_1$  = material constant (0.5 for AF115)

$C_2 = C_2(R, T, f, t_H)$

$C_3 = C_3(R, T, f, t_H)$

$C_4 = C_4(R, T, f, t_H)$

where  $R$  is the stress ratio,  $T$  the temperature,  $f$  the frequency, and  $t_H$  is the hold-time. The model is formulated in an iterative, interactive computer program for computational purposes. If the program is supplied with at least two but no more than eight sets of data in which only one test parameter is varying (e.g. stress ratio) then the SINH model can interpolate for that parameter in the range given with the data. For example, if the program is supplied with three data sets having stress ratios of .1, .5, and .9, then the SINH model will provide the appropriate constants needed for interpolating between these stress ratios. For this example, where all test parameters are constant except for stress ratio ( $R$ ),  $C_2$  through  $C_4$  are only functions of stress ratio. One can then produce an equation for a crack growth rate curve as a function of the stress intensity range  $\Delta K$  for any stress ratio in this range. This SINH model will be described in more detail in the Numerical Analysis section.

The General Electric Company developed a model for predicting crack growth based on a modified sigmoidal

equation (MSE). This equation consists of the products of the exponential and natural logarithmic functions raised to constant powers:

$$da/dN = \exp(B)(\Delta K/\Delta K^*)^P(\ln(\Delta K/\Delta K^*))^Q(\ln(\Delta K_C/\Delta K))^D \quad (2)$$

where

$\Delta K$  = stress intensity range

$\Delta K^*$  = threshold  $\Delta K$  from model

$\Delta K_C$  = critical  $\Delta K$  from model

$B, P, Q, D$  = constants for curve shape.

This model was applied specifically to the material AF115 (nickel-base powder alloy). Thus, this model may not apply as well to other materials. The input for using the MSE model consists of the various test parameters such as the stress ratio, the temperature, the frequency, and the hold-times. The constants for Eq (2) are the output.

Both models use experimental data for AF115 to evaluate their capability to predict crack growth rate behavior. This material is a nickel-base powder super alloy developed by the General Electric Company under Air Force Material Laboratory (AFML) sponsorship (9). AF115 is a creep resistant high strength alloy with operating temperatures up to 1400F. This alloy was designed to be used in high temperature environments where space constraints are

critical. Applications that would meet this criterion would primarily be turbine disks. AF115 is then a prime candidate for the study of high temperature crack growth under cyclic loading with interspersed periods of hold-time loading.

Equations (1) and (2) obtained from the supplied models were numerically integrated for an estimate of the specimen's useful life. Results of the integration were represented as crack length (a) versus number of cycles (N). The integration method was a subroutine supplied by the International Mathematical and Statistical Libraries, Inc. (IMSL) (10). The name of the subroutine is DVERK and uses Runge Kutta methods of orders five and six. The integrated data were plotted along with experimental a versus N data for each loading condition considered. Conclusions were drawn from these plots to determine the accuracy and reliability of each model.

The above discussion outlines the method used to test the SINH and MSE models for crack growth accuracy. Next, this study examined each model's interpretation of crack growth rate ( $da/dN$ ) as a function of hold-time, then, as a function of frequency. Hold-time variation will be used here for illustrating the procedure. The SINH model was supplied with three data sets with hold-times of 0, 90, and 300 seconds. It provided the necessary information needed for interpolating between these hold-times. Several hold-times were then selected so that several crack growth rate equations as a function of the stress intensity range ( $\Delta K$ )

can be produced (see Eq (1)). Fixing the value of  $\Delta K$  generated several values of  $da/dN$ . This crack growth rate data was plotted against the corresponding value of hold-time. This allowed examination of SINH interpretation of crack growth rate as a function of hold-time. The same procedure was used to examine frequency variation. The method of analyzing the MSE model was conducted in a similiar manner.

The MSE model's interpretation of hold-time and frequency effects on crack growth was examined in the following manner. Again hold-time is used for illustration purposes. A hold-time was selected between 0 and 300 seconds. This hold-time was input into the MSE program along with the other constant test parameters. The constants for Eq (2) are the output. Hence, the crack growth rate equation for that hold-time is known. This procedure was repeated for several different hold-times. The resulting set of equations was handled in the same manner as was done with SINH's equations described above.

Another area studied was the ability to predict fatigue-creep crack growth from pure creep data. An empirical model was developed that generated crack growth rate ( $da/dN$ ) data from experimental creep crack growth rate ( $da/dt$ ) data and knowledge of the cyclic wave form. Two wave-forms were considered for this model. Figure 2 illustrates these two wave-forms. The first is composed of loading at a constant rate up to a specific stress

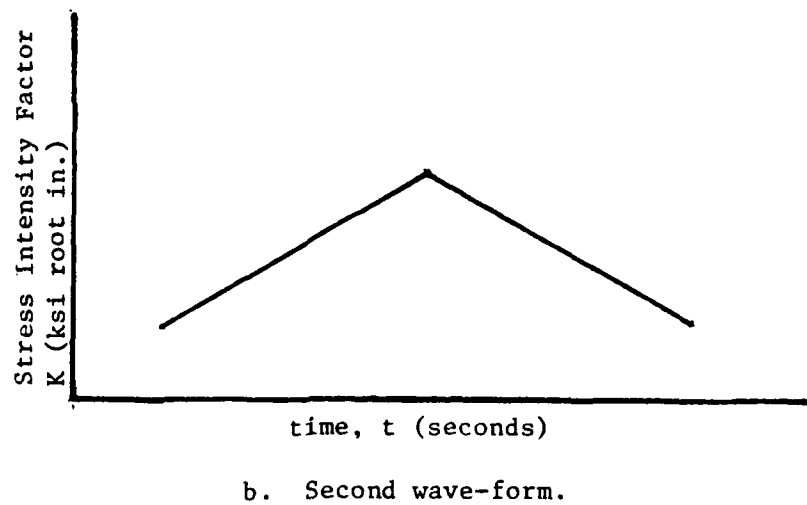
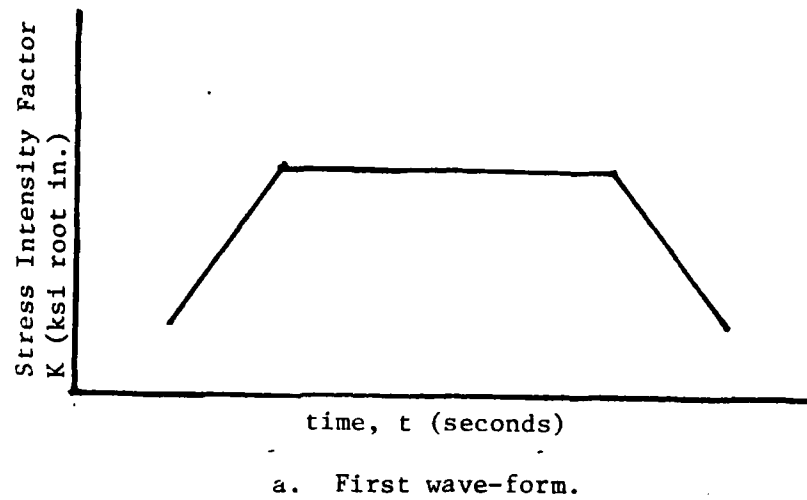


Figure 2. Loading wave-forms selected for study.

intensity, holding that stress for a period of time, then unloading at the same rate. The hold-time at constant load was the changing parameter. The second wave-form consisted of loading at a specified rate, then unloading at the same rate. The rate of loading and unloading was the varying parameter. They were characterized using cycle time. Cycle time is defined to be the time required for either wave form to complete one cycle or period. By varying the cycle time, various values of  $da/dN$  were generated by the model. This  $da/dN$  versus cycle time data was then plotted along with experimental data for analysis of the model's validity. This analysis aided in understanding some interaction effects between fatigue and creep. The data used in this model's development and analysis was supplied by the Air Force Materials Laboratory (AFML)(11;12). This material is Inconel 718, a nickel-base super alloy commonly used in turbine engines. Inconel 718 was chosen for this model development because there was no creep crack growth data available from the AF115 batch. The ability to develop this model and apply it to life predictions is based on the following simplifying assumptions.

The first assumption is that Linear Elastic Fracture Mechanics (LEFM) correctly represents the stress and strain conditions ahead of the crack tip. The equation for the stress intensity factor range ( $\Delta K$ ), used for integrating crack growth rate curves, does not include any plastic zone corrections. Lastly, a power law is the assumed model for

the creep crack growth rate as a function of the stress intensity factor. In this instance, the power law takes the form of Eq (3)

$$da/dt = CK^m \quad (3)$$

where

C,m = empirical constants to be determined  
from experimental data

K = stress intensity factor.

As presented in the results and discussion section, this assumption fits the data reasonably well for the range of stress intensities being considered.

To summarize, two models were used to make specimen life predictions, conclusions were made on each model's accuracy and consistency based on these predictions. The models were used to investigate their ability to predict the effect of hold-time and frequency on crack growth rates. Finally, an empirical model was developed to aid in understanding the effect of fatigue-creep interaction.

### III. Numerical Analysis

Detailed descriptions are presented here of both General Electric's and Pratt and Whitney's models. These models represent the state-of-the art capability for crack growth rate predictions for the aircraft engine industry. The models are discussed in sufficient detail in order to present each model's theoretical foundation and basis for usage. Detailed development for these models are given in (6;7). This section also presents the development of a predictive model to evaluate the ability to use creep data, along with knowledge of the wave-form, to predict fatigue-creep crack growth rates.

#### The Pratt and Whitney (SINH) Model

The interpolative hyperbolic sine model (SINH) is a mathematical tool which provides crack propagation rate as a function of various parameters. Pratt and Whitney selected the hyperbolic sine equation to represent crack growth rate ( $da/dN$ ) as a function of the stress intensity range ( $\Delta K$ ) for the following reasons:

1. It exhibits the overall sigmoidal shape of typical  $da/dN$  versus  $\Delta K$  plots as shown in Figure 1.
2. All or part of the equation may be used to fit data. Also, the slope at the inflection can be adjusted with the fitting constants.
3. The hyperbolic sine is not periodic nor asymptotic (e.g. trigonometric tangent); therefore when extrapolation becomes necessary, the sinh behaves well at distances removed from data.

The SINH model is based on the hyperbolic sine function and is given as

$$\log(da/dN) = C_1 \sinh(C_2(\log(\Delta K) + C_3)) + C_4 \quad (4)$$

where the constants have been shown (15; 16; 17) to be functions of the test frequency, the stress ratio, and the temperature for pure cyclic loading:

$C_1$  = material constant (0.5 for AF115)

$C_2 = C_2(f, R, T)$  = shape factor

$C_3 = C_3(f, R, T)$  = abscissa of the inflection point  
( $-\log \Delta K$ )

$C_4 = C_4(f, R, T)$  = ordinate of the inflection point  
( $\log(da/dN)$ )

where  $f$  is the frequency,  $R$  the stress ratio and  $T$  the temperature. For interpolating in regions where there are no data, the constants  $C_2$ - $C_4$  are assumed linear functions of the crack growth parameters as specified below

$$C_2 = a + b * FNCTN$$

$$C_4 = c + d * FNCTN \quad (5)$$

$$C_3 = e + f * C_4$$

FNCTN is a function of the individual test parameter which is being regressed. Table 1 defines these relationships. These relationships allow development of an interpolative model of crack propagation as a function of any one test

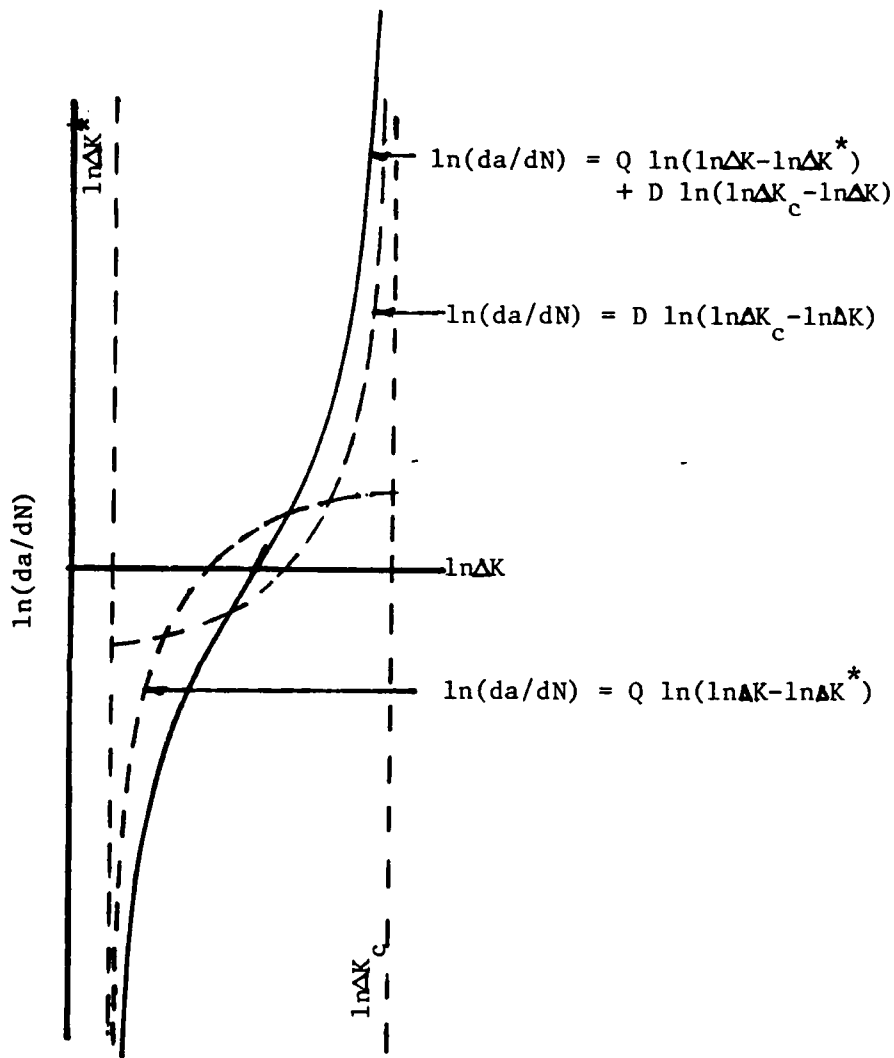
Table 1. Functional Relationships for the Test Parameters

| Test Parameter      | FNCTN              |
|---------------------|--------------------|
| Stress Ratio (R)    | $\text{Log}(1-R)$  |
| Frequency (f)       | $\text{Log}(f)$    |
| Temperature (T)     | T                  |
| Hold-Time ( $t_H$ ) | $-\text{Log}(t_H)$ |

parameter. Because of the simple relationships observed between the coefficients of the SINH model and the basic crack propagation controlling parameters, interpolations are straight forward. It is here that the usefulness of the model is best demonstrated; the SINH model provides descriptions of crack propagation characteristics even in regions where data are unavailable. Appendix A gives a basic development of the SINH model. For a detailed development see (7).

#### The General Electric's (MSE) Model

The development of General Electric's model is based on the introduction of a sigmoidal equation which had the flexibility of correlating the complete range of conventional cyclic crack growth rate versus stress intensity range data. The interpolative model was developed using a modified form of a sigmoidal equation (MSE) given in Eq (2). The lower and upper asymptotes are expressed by  $\Delta K^*$  and  $\Delta K_c$ , respectively. The coefficients Q and D are shaping coefficients that control the lower and upper section of the sigmoidal curve (see Figure 3). Decreasing the absolute value of D or Q results in a sharper transition at the appropriate end of the curve. The coefficient P in the MSE allows control of rotation at the inflection point of the crack growth curve. Changing the B coefficient results in a vertical movement of the curve. The horizontal location of the inflection point is determined by a mathematical combination of  $\Delta K^*$ ,  $\Delta K_c$ , D, and Q (6:37).



$$B = P = 0 \text{ and } D = -Q$$

Figure 3. Upper and Lower Shaping Method of the Sigmoidal Model.

The six coefficients ( $B, P, Q, D, \Delta K^*$ , and  $\Delta K_c$ ) are related to temperature, stress ratio, frequency and hold-time. Some of the coefficients interact with only one or two of the four test variables. Others, such as the ones used for locating the inflection point are more complex and are related to all four test variables (6:37). In many situations during the development of this model by General Electric, the coefficients governing the crack growth curve were estimated since tests were not conducted at all possible combinations of the four test variables. The estimates were achieved by considering the surrounding test results in which only one test variable was different from that being examined. Details of each of the derived relationships are given in (6:38-51).

The derivation of the model was based essentially on examining how the  $da/dN$  versus  $\Delta K$  curves changed with a change in test parameter. The experimental data were then incorporated into the MSE model through the six coefficients. These coefficients are functions of the test parameters; therefore, changing the test parameters would change the six constants which in turn would alter the shape of the MSE. Modeling of the upper and lower asymptotes will be presented as examples of the derivation technique. These derivations are taken from (6:38-39) and are based on AF115.

The final crack length was measured from each of the failed specimens and the stress intensity range was calculated based on the crack length and the applied loads.

No correlation of the final stress intensity range to frequency, hold-time, or temperature was found. On the other hand, the final stress intensity range did depend on stress ratio; this relationship may be written as follows:

$$\Delta K_c = \Delta K_{\max}(1-R) \quad (6)$$

The value of  $\Delta K_{\max}$  was calculated to be 122 ksi (in)<sup>1/2</sup>.

The lower asymptote  $\Delta K^*$ , was estimated from each set of da/dN versus  $\Delta K$  data. It was found to be dependent on the stress ratio and the temperature and independent of the frequency and the hold-times. For the stress ratio of 0.1 and temperatures between 1000 and 1400 F,  $K^*$  was estimated as 10 ksi (in)<sup>1/2</sup>. When plotted versus (1-R) on logarithmic coordinates, as done by General Electric (6:39), linear relationships were observed for each temperature (see Figure 4) so that:

$$\Delta K^* = \Delta K^*_{\max}(1-R)^2 \quad (7)$$

For each temperature,  $\Delta K^*_{\max}$  is the intercept at the stress ratio of zero, and n is the slope. They were related to temperature by:

$$n = a_1 + b_1(T - 1000)^d$$

$$\Delta K^*_{\max} = a_2 + b_2(T-1000)^e$$

where  $a_1$ ,  $a_2$ ,  $b_1$ ,  $b_2$ ,  $d$ , and  $e$  are constants determined by simple regression analysis (Figure 4).

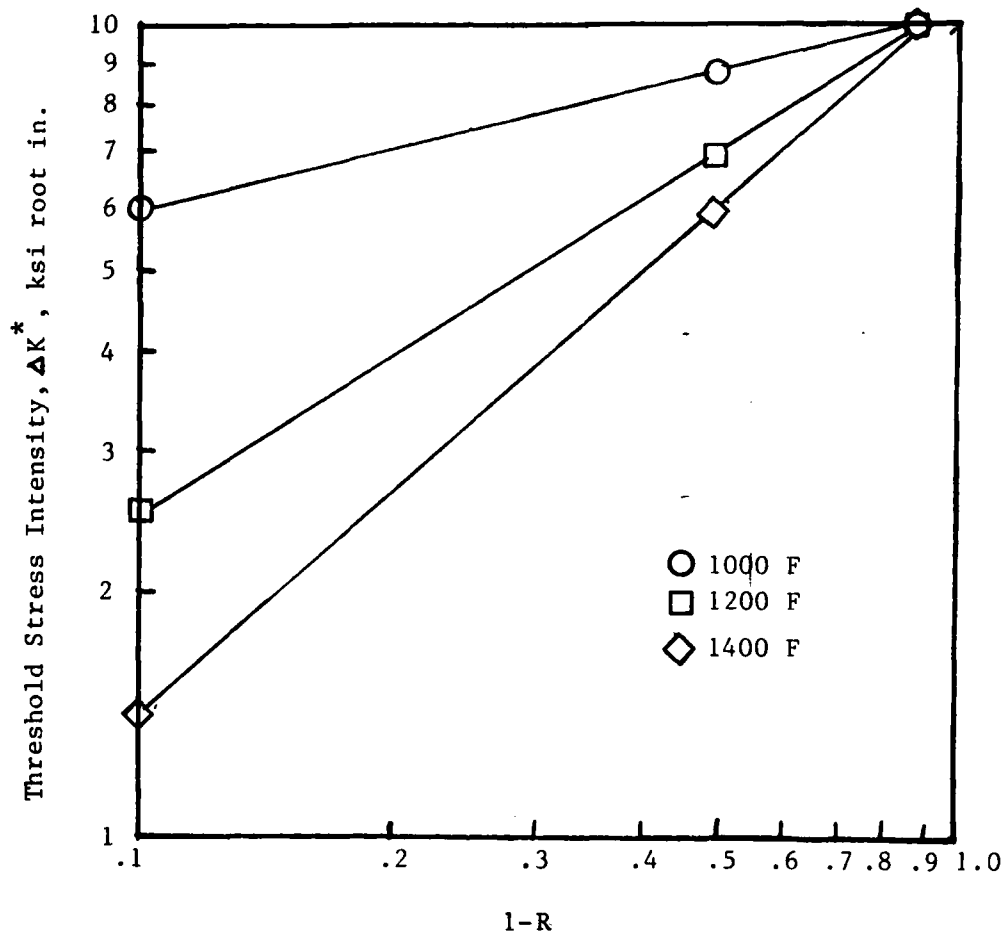


Figure 4. Correlation of Threshold Crack Growth and Stress Ratio (1-R) for 1000, 1200, and 1400 F.

A summary of the coefficients influenced by the four test parameters are given by General Electric (6:53) and reproduced here in Table 2. These coefficients are used to evaluate the constants in the MSE model.  $\Delta K_i$  and  $da/dN_i$  are used to evaluate B. Also,  $da/dN_i$  was used to find the slope of the curve at the inflection point (P) (6:37). The upper shaping parameter (D) is not listed in Table 2, because it is calculated knowing Q,  $\Delta K_i$ ,  $\Delta K_{c1}$  and  $\Delta K^*$  (6:37). Complete derivations of these six coefficients are given in (6). Appendix B presents the computer code for the MSE model used in this study. This code is an updated version of the code listed in the appendix of (6).

#### Predictive Model

Presented here is the development of a predictive model to examine the ability to predict fatigue-creep crack growth from creep data and knowledge of the wave-form. Modeling of the experimental creep data was the first step of development. The creep crack growth rate data used in this analysis is shown in Figure 5. For the stress intensity ranges used in this study, creep crack growth rate data from Inconel 718 can be represented by a linear relationship on logarithmic coordinates. The equation which expresses creep crack growth rate as a function of stress intensity factor is

$$da/dt = CK^m \quad (9)$$

Table 2. Influence of Experimental Parameters on the Sigmoidal Model Coefficients.

|              | Temperature | Frequency | Hold-Time | Stress Ratio |
|--------------|-------------|-----------|-----------|--------------|
| $\Delta K_c$ |             |           |           | X            |
| $\Delta K^*$ | X           |           |           | X            |
| $\Delta K_i$ | X           | X         | X         | X            |
| $da/dN_i$    | X           | X         | X         | X            |
| $da/dN'_i$   | X           | X         | X         | X            |
| Q            | X           |           |           | X            |

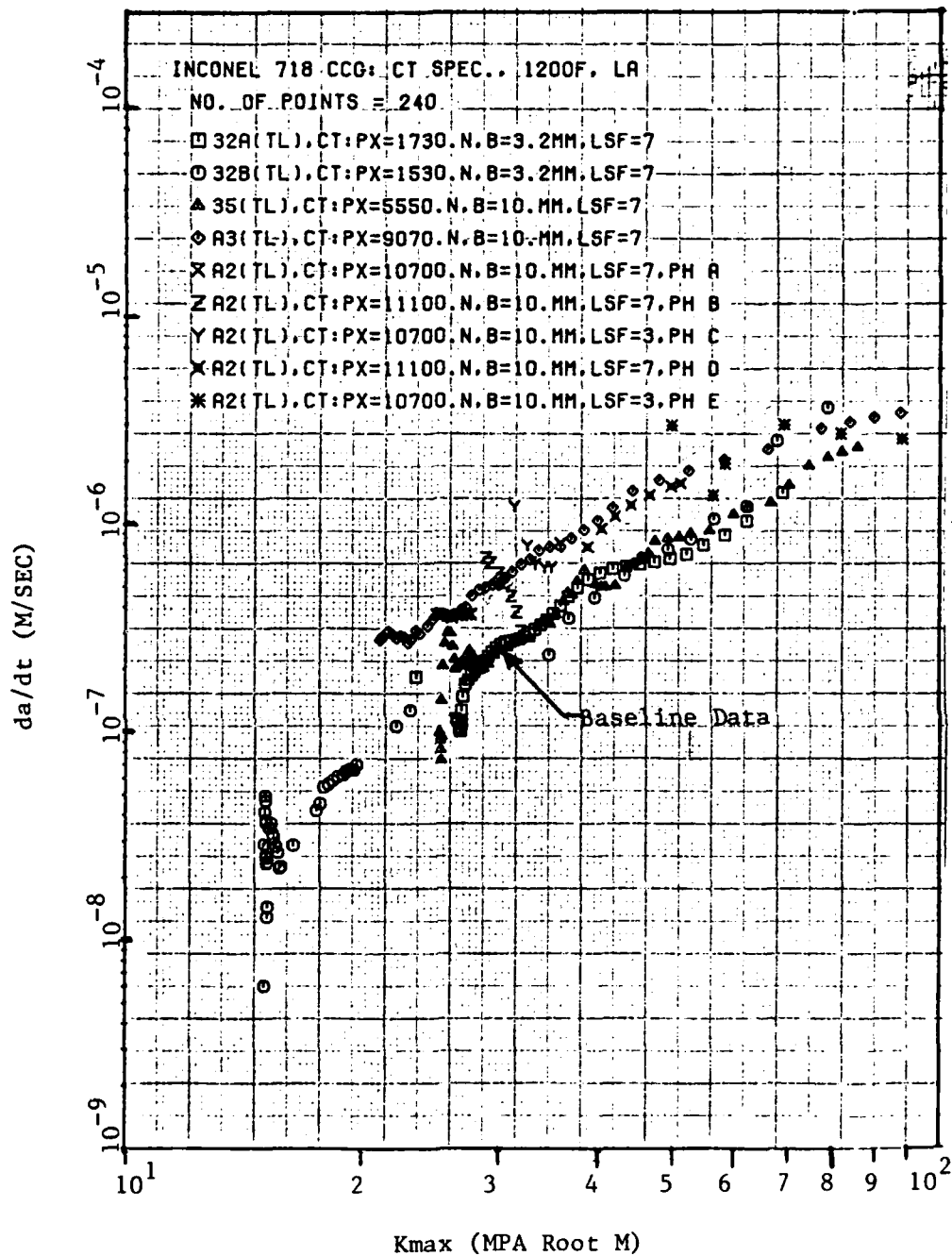


Figure 5. Maximum Stress Intensity Factor  $K_{max}$ , versus the Creep Crack Growth Rate  $da/dt$ , for Inconel 718 at 1200 F.

where

K = stress intensity factor

m = slope of fitted line

C = conversion constant

The constants C and m are determined by fitting a straight line to the baseline data in Figure 5 over the range of K values being considered.

Two loading wave-forms were selected to evaluate the analytical model and are presented in Figure 6. The frequency of the ramps and the magnitude of the hold-times are variable. Wave-form (b) is equivalent to wave-form (a) when the hold-time is zero, and can be considered to be a subset of (a). The first wave-form is divided into three parts as shown in Figure 6. This wave-form may be expressed as a function of time and the loading parameters. These equations are given as follows

for part 1:

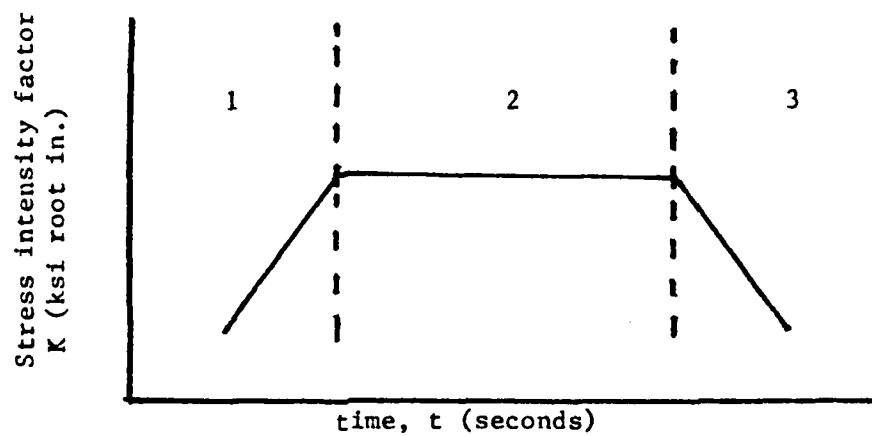
$$K(t) = \Delta K r / (1-R) + 2 \Delta K f_1 t \quad \text{from } t=0 \text{ to } t=1/2 f_1 \quad (10)$$

for part 2:

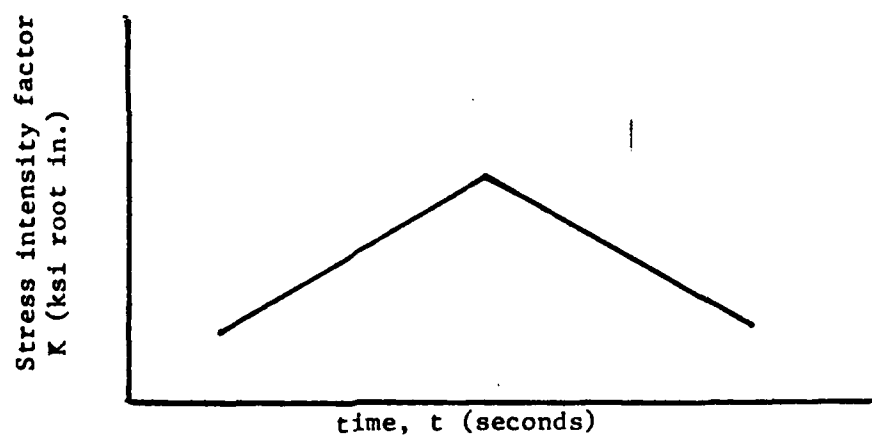
$$K(t) = \Delta K / (1-R) = \text{constant} \quad (11)$$

for part 3:

$$K(t) = \Delta K / (1-R) - 2 \Delta K f_u t \quad \text{from } t=0 \text{ to } t=1/2 f_u \quad (12)$$



a. Varting hold-time wave-form.



b. Varying frequency wave-form.

Figure 6. Loading wave-form selected for study.

where

$\Delta K = K_{\max} - K_{\min} = \text{stress intensity range}$

$R = K_{\min}/K_{\max} = \text{stress ratio}$

$f_1 = \text{loading rate (cycles/second)}$

$f_u = \text{unloading rate (cycles/second)}$

$t_H = \text{hold-time (seconds)}$

Eqs (10)-(12) are substituted into Eq (9) and analytically integrated for one complete cycle, namely for part 1:

$$\int_0^{a_1} da = \int_0^{1/2f_1} C(\Delta KR/(1-R) + 2\Delta Kf_1t)^m dt \quad (13)$$

for part 2:

$$\int_0^{a_2} da = \int_0^{t_H} C(\Delta K/(1-R))^m dt \quad (14)$$

for part 3:

$$\int_0^{a_3} da = \int_0^{1/2f_u} C(\Delta K/(1-R) - 2\Delta Kf_u t)^m dt \quad (15)$$

If  $m \neq -1$  then integration yields

for part 1:

$$a_1 = C \left[ \frac{(\Delta KR/(1-R) + \Delta K)^{m+1} - (\Delta KR/(1-R))^{m+1}}{2(m+1)\Delta Kf_1} \right] \quad (16)$$

for part 2:

$$a_2 = C(\Delta K/(1-R))^m t_H \quad (17)$$

for part 3:

$$a_2 = C \left[ \frac{\Delta K - \Delta K/(1-R)^{m+1} + (\Delta K/(1-R))^{m+1}}{2(m+1)\Delta K f_u} \right] \quad (18)$$

The result of the integration is the amount of crack growth in one loading cycle. This is defined as the fatigue-creep cyclic crack growth rate

$$da/dN = a_1 + a_2 + a_3 \quad (19)$$

Equation (19) can be used to predict fatigue-creep crack growth rates from creep data and knowledge of the wave-form. This equation was programmed into a computer whose inputs are the creep data, and the loading wave-form parameters defined in Eq (12). The program fits a straight line to the creep crack growth data to produce the constants C and m. With these constants and the wave-form parameters, the program will return a value for the cyclic crack growth rate (da/dN). Calculations were conducted for a range of values of the wave-form parameters. The calculated values of da/dN were compared to experimental data on Inconel 718. The comparisons are presented in the Results and Discussion Section.

#### IV. Results and Discussion

Data were collected on AF115 from a contract sponsored by the Air Force Wright Aeronautical Laboratories (6). All cyclic crack growth experiments were conducted at General Electric, Aircraft Engine Group (AEG), in two servo-controlled electrohydraulic test systems operated under closed-loop control. Details on specimen fabrication, precracking, heating, crack measuring, and data reduction are given in Appendix C. For more information on this material see (6:2-23).

Results of crack growth comparisons of the MSE and SINH models are shown in Figures 7 through 9. Each graph is composed of integrated crack growth rate curves from each model and experimental data for that loading condition. Notice that for clarity the abscissa of Figure 7 is expanded with respect to Figures 8 and 9. The crack growth rate curves along with the experimental data used for curve fitting are plotted in Figures 10 and 11. The equations used to produce these curves are given below each graph. The equations for the SINH model shown in Figure 10 were arrived at by producing an interpolative model for hold-time. Hold-times of 0, 90, and 300 seconds were chosen and the constants  $C_2$  through  $C_4$  were calculated. The process employed by the SINH model to arrive at this interpolative model was discussed in the Numerical Analysis Section. The

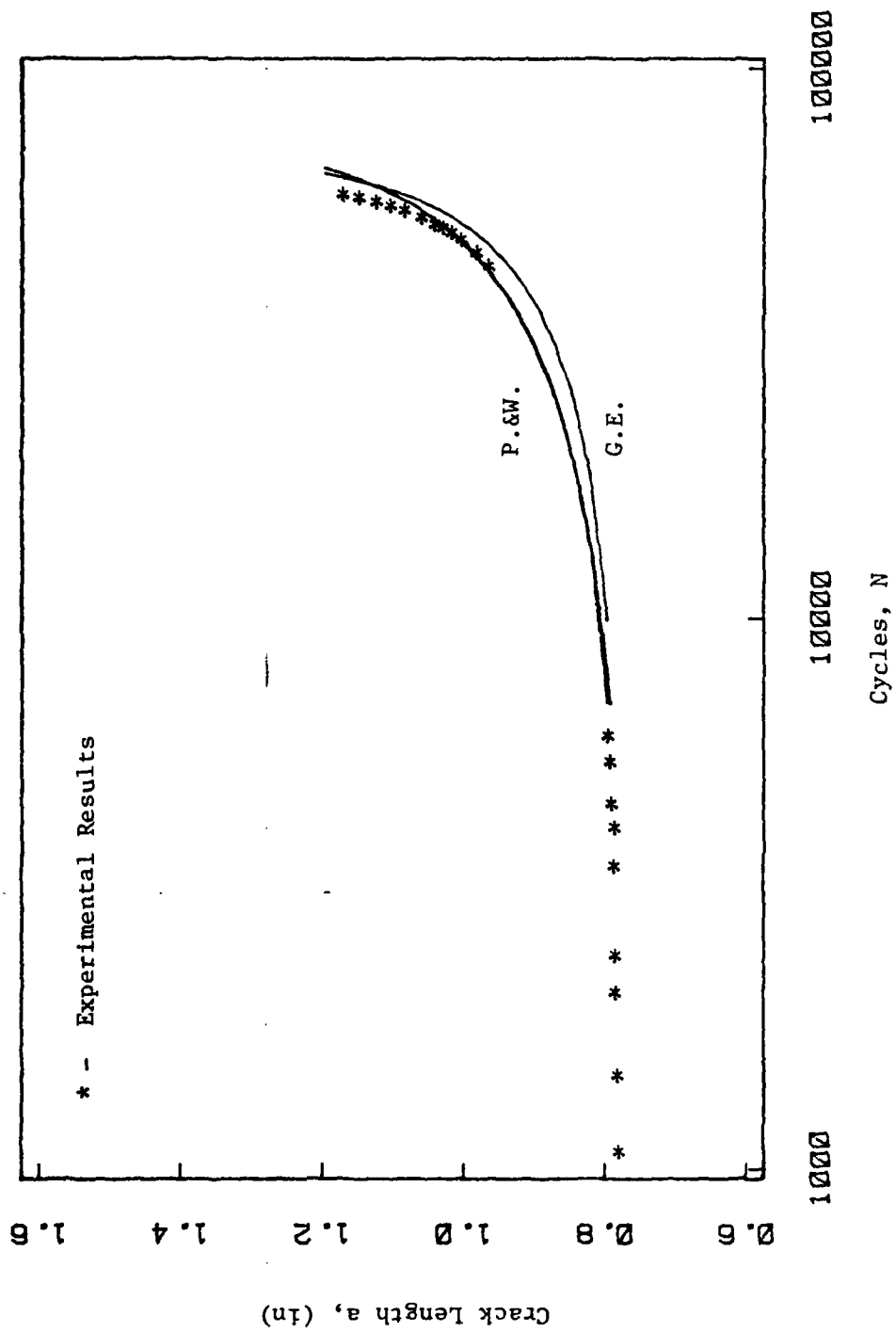


Figure 7. Comparison plot of AF115 for  $R = .1$ ,  $T = 1200$  F,  $f = .25$  Hz, and  $t_H = 0$  sec.

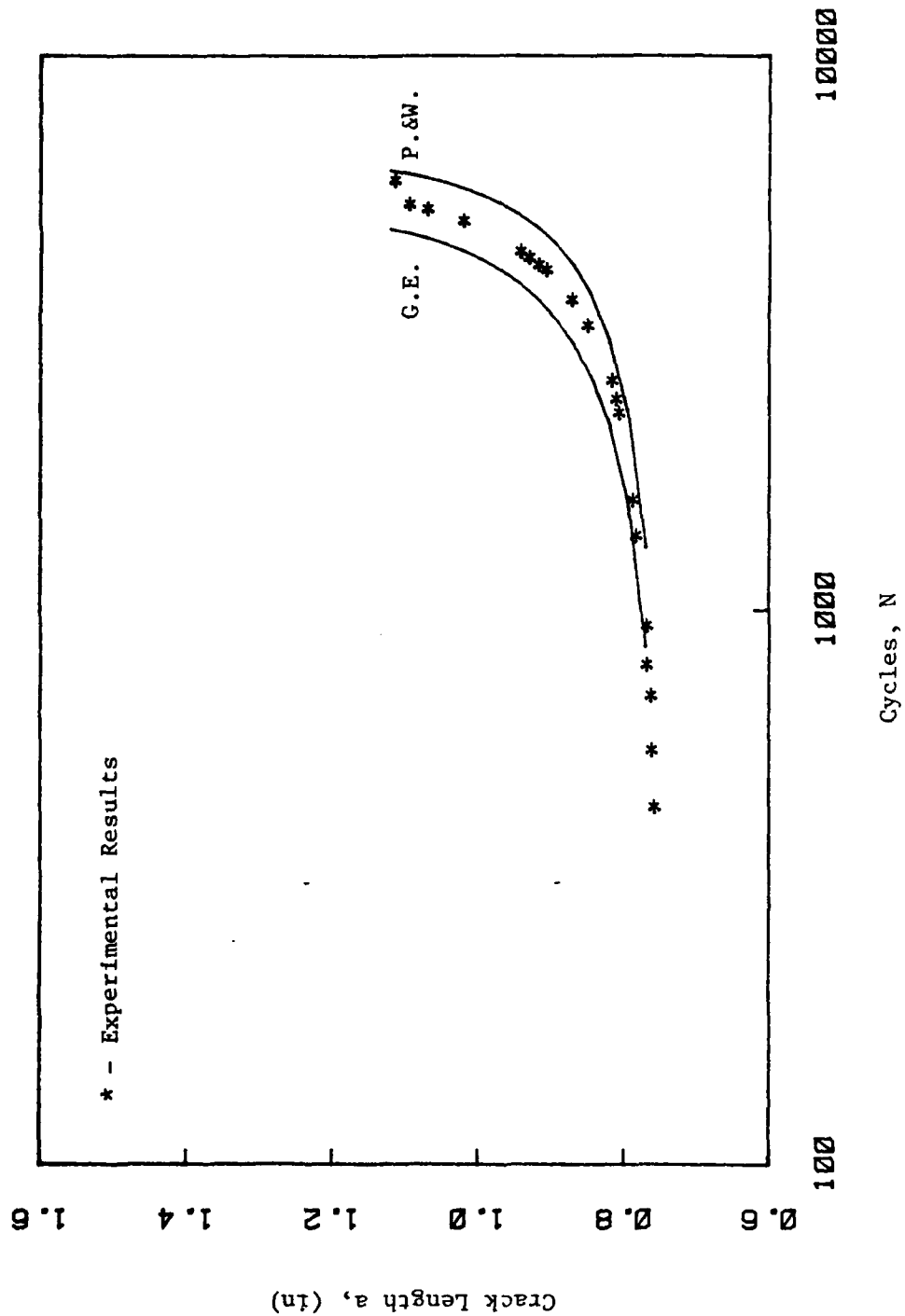


Figure 3. Comparison plot of AF115 for  $R = .1$ ,  $T = 1200$  F,  $f = .25$  Hz, and  $t_H = 90$  sec.

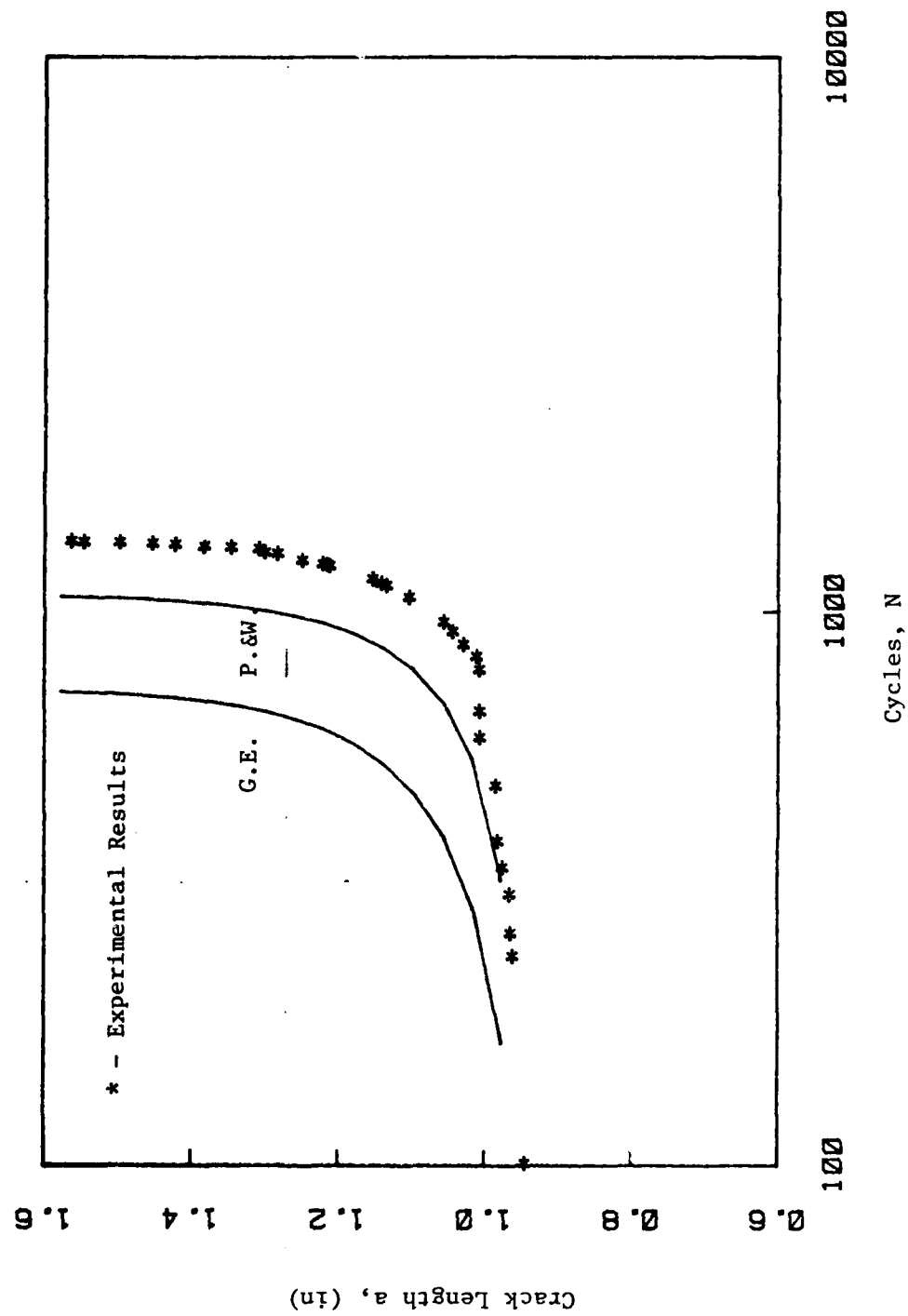
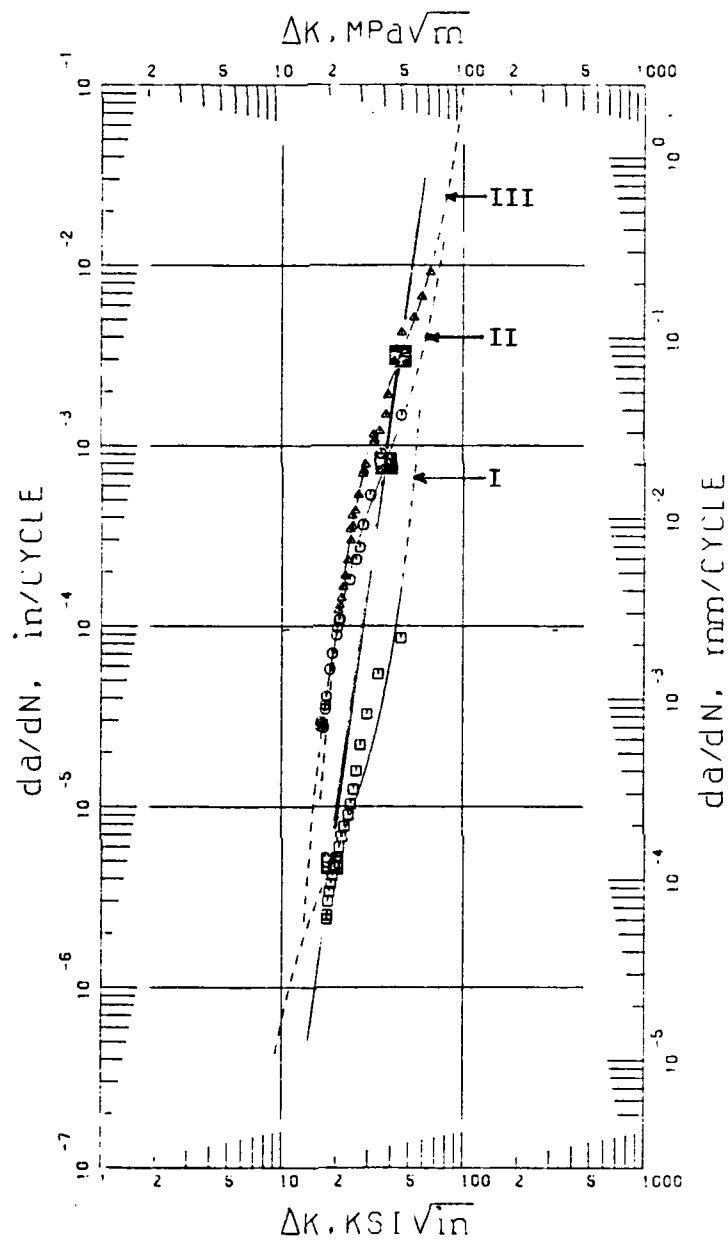
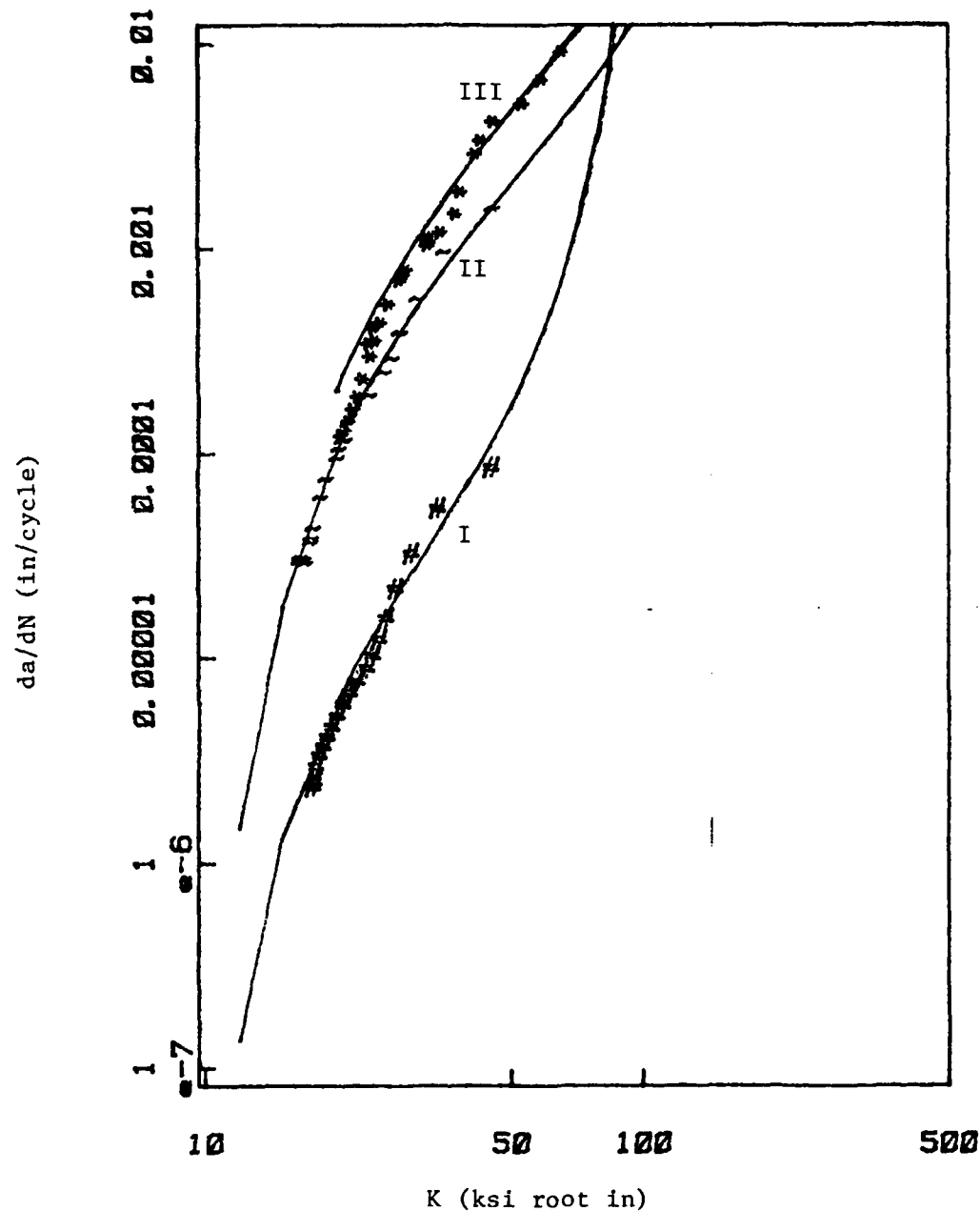


Figure 9. Comparison plot of AF115 for  $R = .1$ ,  $T = 1200$  F,  $f = .25$  Hz, and  $t_H = 300$  sec.



- I.  $\text{Log}(da/dN) = 0.5\sinh(4.787(\log(\Delta K) - 1.276)) - 5.315$   $t_H = 0.0s$
- II.  $\text{Log}(da/dN) = 0.5\sinh(5.146(\log(\Delta K) - 1.573)) - 3.100$   $t_H = 90.0s$
- III.  $\text{Log}(da/dN) = 0.5\sinh(5.242(\log(\Delta K) - 1.652)) - 2.508$   $t_H = 300.0s$

Figure 10. Stress Intensity Range  $\Delta K$ , versus Crack Growth Rate  $da/dN$ , using SINH Model for AF115 Data.  
 $R = .1$ ,  $T = 1200$  F,  $f = .25$  Hz.



- I.  $da/dN = \exp(-7.36) (\Delta K/10)^{-2.27} (\ln(\Delta K/10))^{3.00} (\ln(109.8/\Delta K))^{-3.69}$
- II.  $da/dN = \exp(-7.99) (\Delta K/10)^{.15} (\ln(\Delta K/10))^{3.00} (\ln(109.8/\Delta K))^{-.47}$
- III.  $da/dN = \exp(-7.61) (\Delta K/10)^{.46} (\ln(\Delta K/10))^{3.00} (\ln(109.8/\Delta K))^{-.23}$

Figure 11. Stress Intensity Range  $\Delta K$ , versus Crack Growth Rate  $da/dN$ , using MSE Model for AF15 Data.  $R = .1$ ,  $T = 1200$  F, and  $f = .25$  Hz.

constants used in the MSEs model presented in Figure 11 are obtained by substituting the test parameters into the MSE computer program. The test parameters used are presented with each figure. Note that as the hold-time increases from 0 seconds (Figure 7), to 90 seconds (Figure 8), and to 300 seconds (Figure 9) the number of cycles to failure decreases; also note that the predicted curves begin to deviate from the experimental data. Table 3 illustrates this deviation by presenting the ratio of the predicted number of cycles to failure (P) to the actual number of cycles to failure (A). A value for P/A less than 1.0 indicates a conservative estimate whereas a value greater than 1.0 suggests an unconservative estimate of crack growth.

Besides investigating each model's capability to predict crack growth curves, each model was also examined for its ability to interpret the variation of the crack growth rate with a changing test parameter. Two test parameters were considered; hold-time and frequency. Considering hold-time variation first, Figures 12 and 13 represent each model's interpretation of crack growth rate variation with hold-time. The stress intensity factor range,  $\Delta K$ , along with the other test parameters and values of  $da/dN$  were computed for various hold-times from each model. The method used to compute this data is presented in the Approach section. The test parameters held fixed are the stress ratio, frequency, and temperature with values of 0.1, 0.25 Hertz, and 1200 F respectively. The two  $\Delta K$  values

Table 3. Comparison of Predicted to Actual  
Number of Cycles to Failure.

| Model   | Hold-time<br>(seconds) | $\frac{\text{Predicted } N}{\text{Actual } N}$ |
|---------|------------------------|--|
| P. & W. | 0.0                    | 1.1093   |
|         | 90.0                   | 1.0405   |
|         | 300.0                  | 0.7913   |
| G. E.   | 0.0                    | 1.0855   |
|         | 90.0                   | 0.8146   |
|         | 300.0                  | 0.5338   |

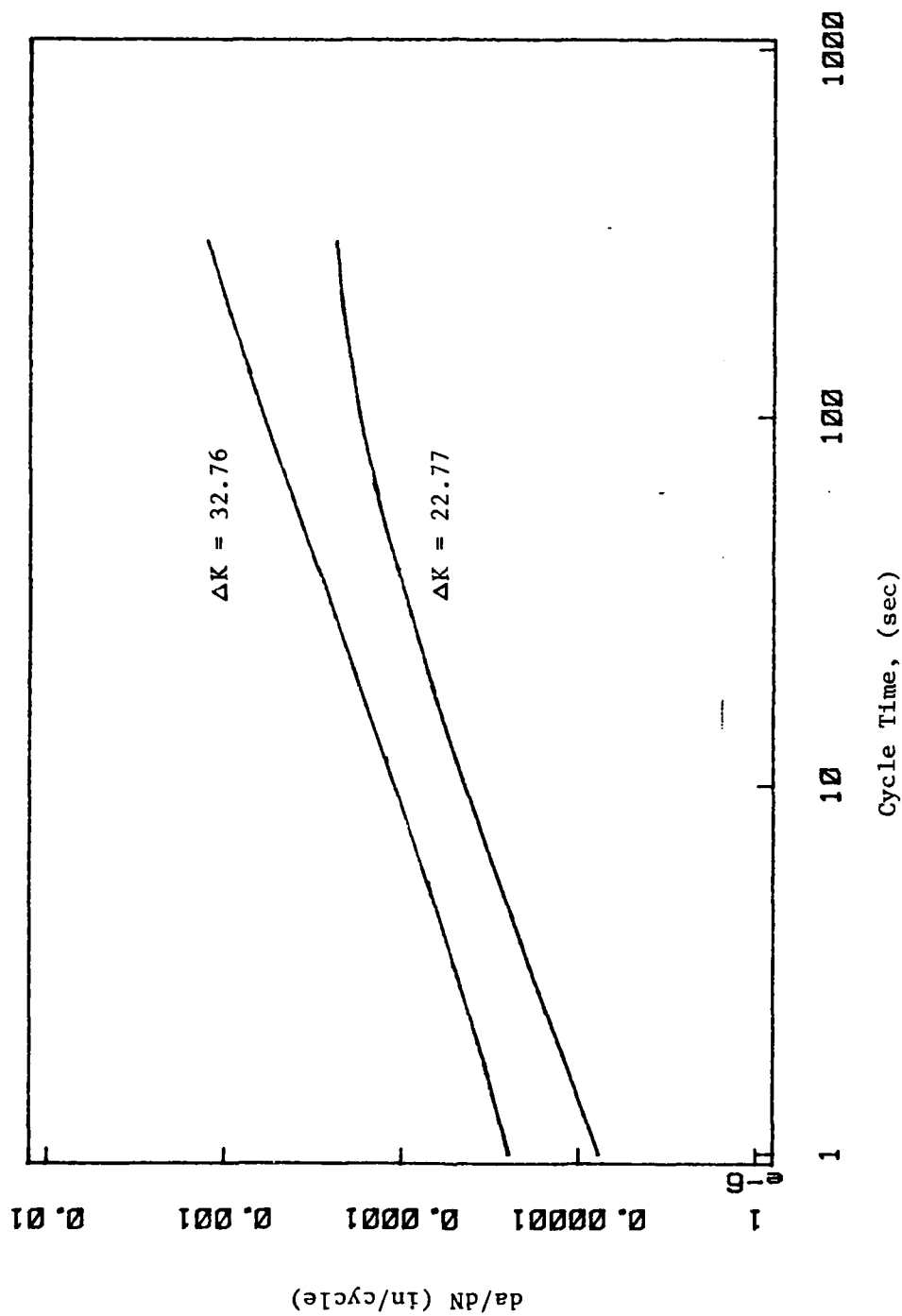


Figure 12. SINH Model interpretation of Crack Growth Rate,  $da/dN$  with hold-time at two loads.

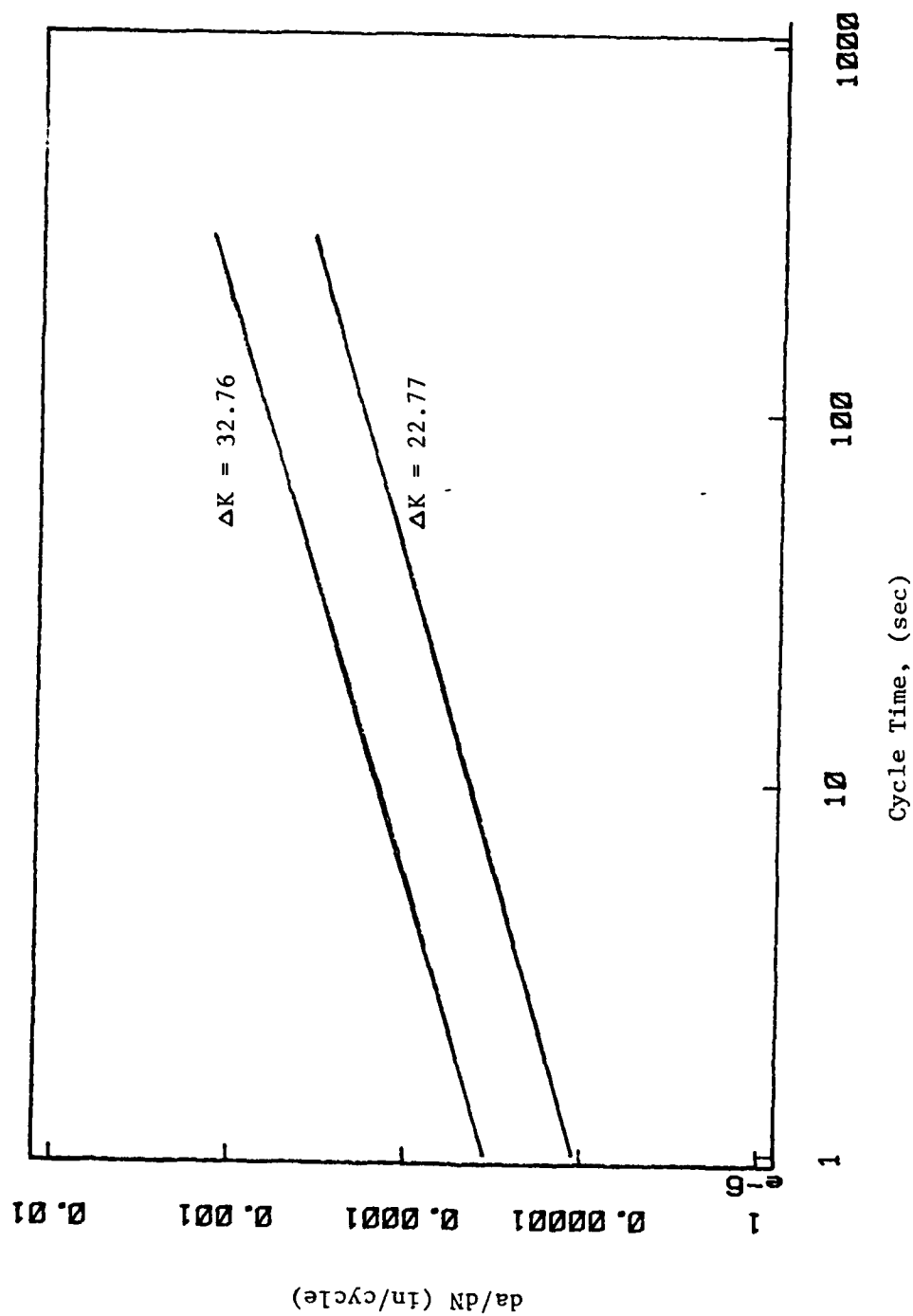


Figure 13 MSE Model interpretation of Crack Growth Rate,  $da/dN$  with hold-time at two loads.

selected were 22.77 and 32.76 ksi (in)<sup>1/2</sup>. The wave-form described by these test conditions is illustrated in Figure 6a. The SINH model shows some nonlinearity for the lower load ( $\Delta K$ ) (Figure 12) whereas the MSE model appears linear for both loads (Figure 13). Considering now the frequency variation and using the same procedure to compute data as with the hold-time variation, the results shown in Figures 14 and 15 were obtained. A hold-time of 0 seconds was chosen in this case. All other test parameters are equivalent to the hold-time test. The wave-form described by these test conditions is presented in Figure 6b. In Figure 14, the SINH model presents a very nonlinear interpretation of crack growth rate variation with frequency for the data used. This model seems to suggest that at a  $\Delta K$  of 22.77 Ksi (in)<sup>1/2</sup> the crack growth rates actually decrease with some values of frequency. The MSE model's interpretation, illustrated in Figure 15, consists of parallel horizontal lines for the two loads considered. Figures 16 and 17 present experimental data on AF115 and the curves fitted to this data by each model. AF115 data with frequency varying between each data set was incorporated into each model so that interpolative results on frequency variation could be obtained.

For comparison with actual data on another material, Figure 18 shows experimental data on Inconel 718. This figure was produced at the Air Force Materials Laboratory (11). This material was tested under the same conditions as AF115 whose computer generated data are

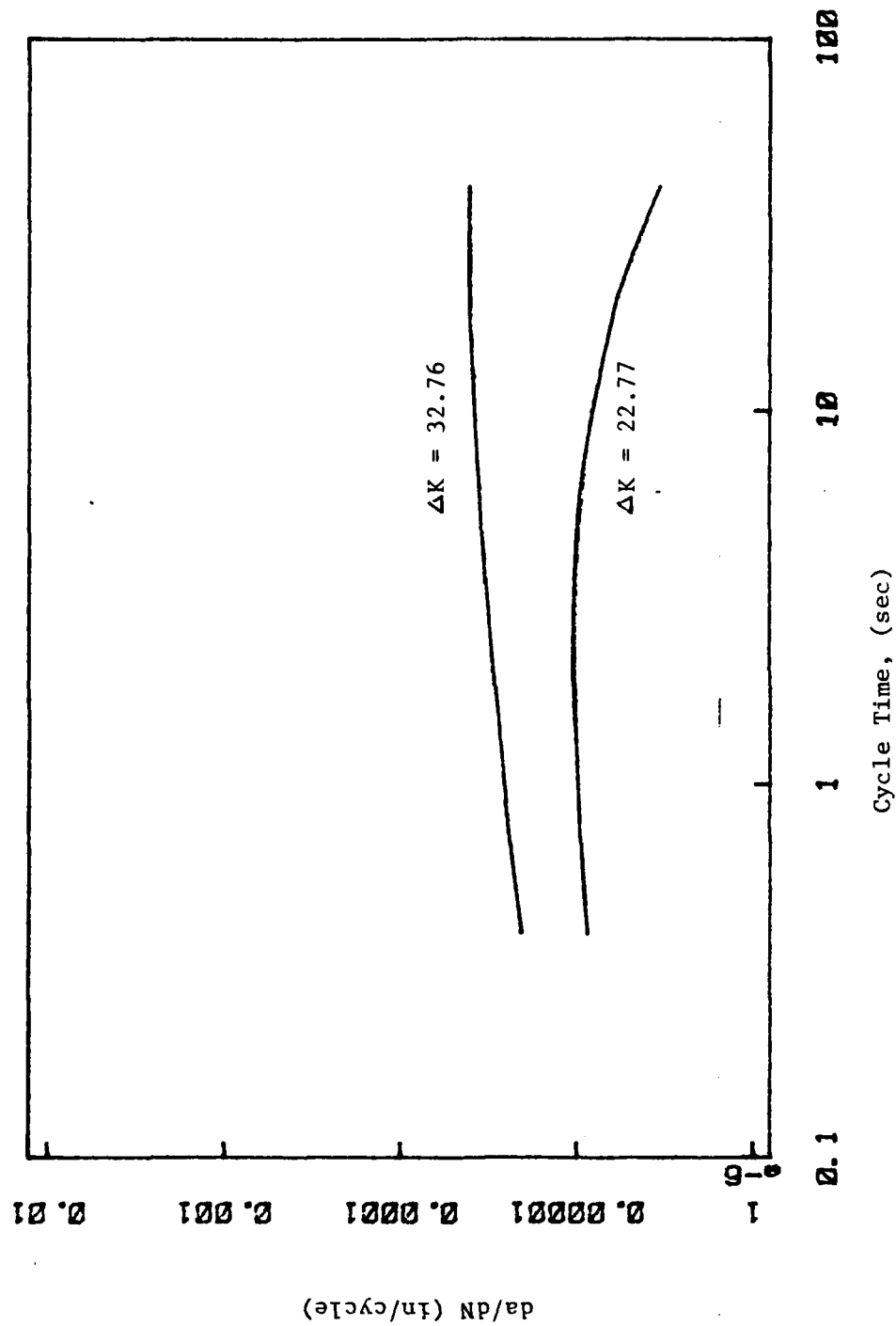


Figure 14. SINH Model Interpretation of Crack Growth Rate,  $da/dN$  with frequency at two loads.

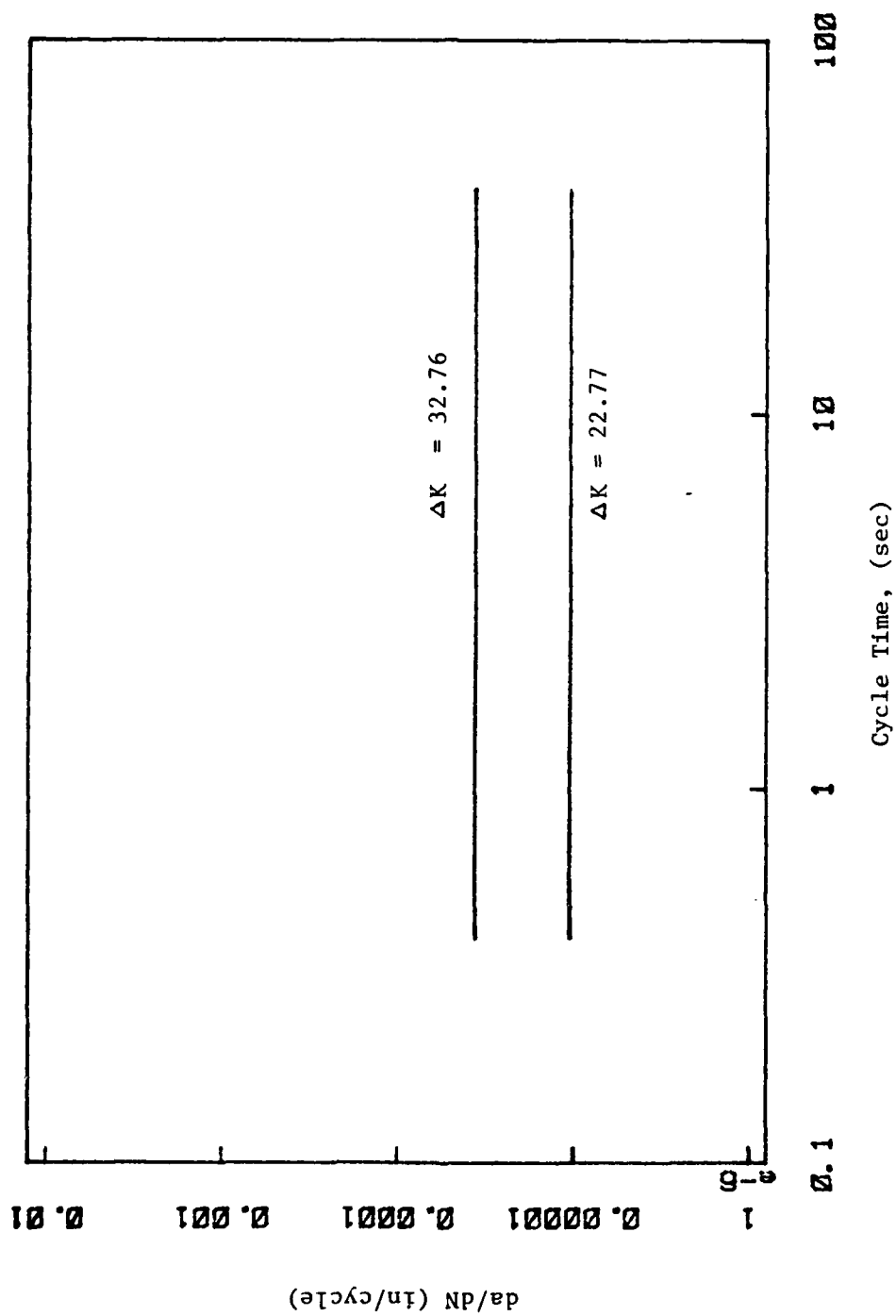
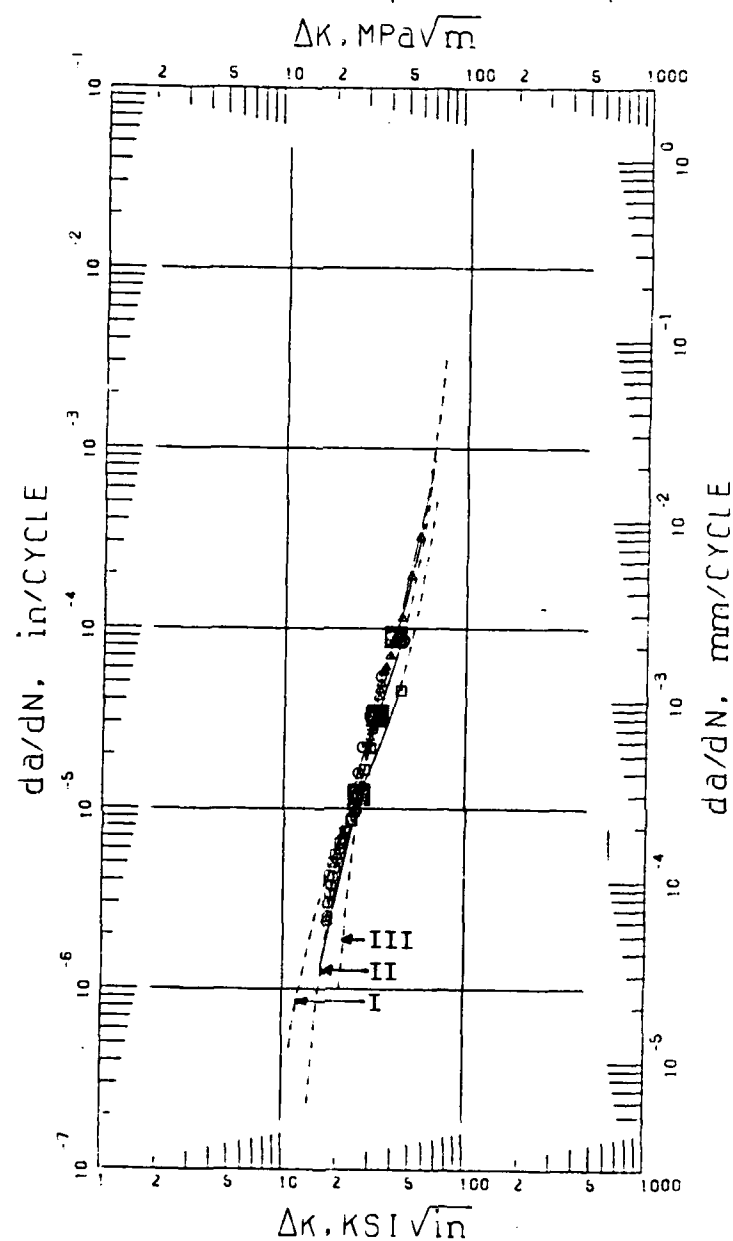
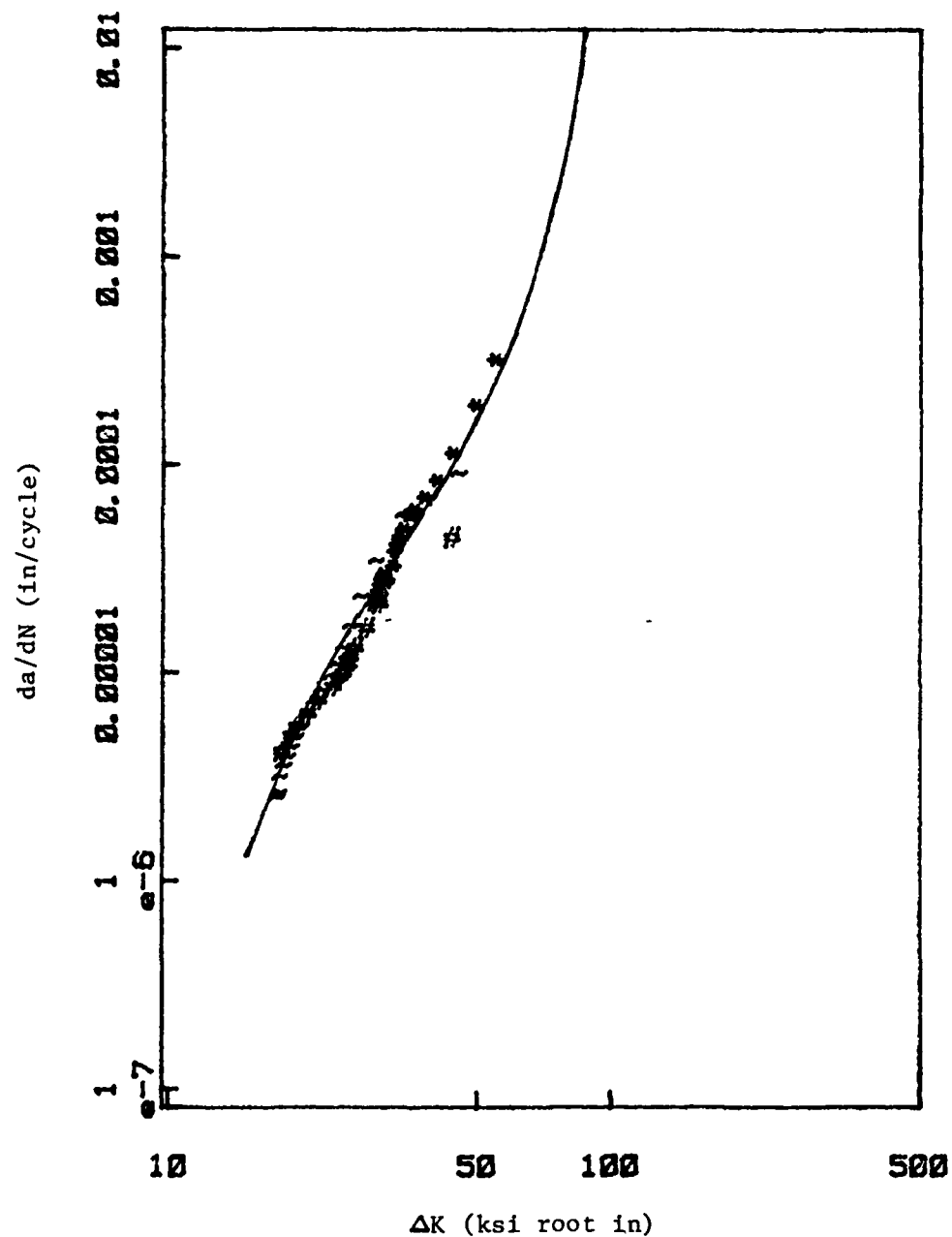


Figure 15. MSE Model Interpretation of Crack Growth Rate,  $da/dN$  with frequency at two loads.



- I.  $\text{Log}(da/dN) = 0.5\sinh(4.691(\log(\Delta K)-1.417))-4.924$   $f = 2.5 \text{ Hz}$   
 II.  $\text{Log}(da/dN) = 0.5\sinh(5.838(\log(\Delta K)-1.513))-4.466$   $f = .25 \text{ Hz}$   
 III.  $\text{Log}(da/dN) = 0.5\sinh(7.046(\log(\Delta K)-1.609))-4.048$   $f = 0.25 \text{ Hz}$

Figure 16. Stress Intensity Range  $\Delta K$ , versus Crack Growth Rate  $da/dN$ , using SINH Model for AF115 Data.  
 $R = .1$ ,  $T = 1200 \text{ F}$ ,  $t_H = 0.0 \text{ sec}$ .



$$da/dN = \exp(-7.36) (\Delta K/10)^{-2.77} (\ln(\Delta K/10))^{3.0} (\ln(109.8/\Delta K))^{-3.69}$$

Figure 17. Stress Intensity Range  $\Delta K$ , versus Crack Growth Rate  $da/dN$ , using the MSE Model for AF115 Data.  
 $R = .1$ ,  $T = 1200$  F,  $t_H = 0.0$  sec,  $f = 2.5-.025$  Hz

represented by Figures 12 through 15. Figure 18 illustrates the experimental crack growth rate variation with cycle time for nickel-base super alloy 718. The dashed and solid curves in Figure 18 correspond to the loading wave-forms shown in Figure 6a and 6b respectively. This experimental data was used to examine the prediction ability of Eq (19). The results of this analysis follow.

Figure 19 illustrates the accuracy of Eq (19) in predicting fatigue-creep crack growth rates. Figure 5 presents the creep data on Inconel 718 used to determine the constants  $C$  and  $m$  in Eq (19). The baseline data were selected for curve fitting. Figure 19a presents the results of using Eqs (19) and the loading wave-form shown in Figure 6a. Figure 19b presents the results of using Eq (19) and the loading wave-form shown in Figure 6b. For Figure 19b, Eq (19) and experimental data are almost identical for cycle times greater than 5 seconds. In Figure 19b the upper straight line was obtained by integrating the entire associated wave-form. The lower straight line is the result of only integrating half the wave-form shown in Figure 19b. Note that the lower straight line is a better approximation to the experimental data shown in Figure 19b. Also note that the break in the bilinear lines from Figure 19a to 19b is shifted to the right by about an order of magnitude. This change in slope corresponds to a transition from predominantly fatigue crack growth to mostly creep crack growth.

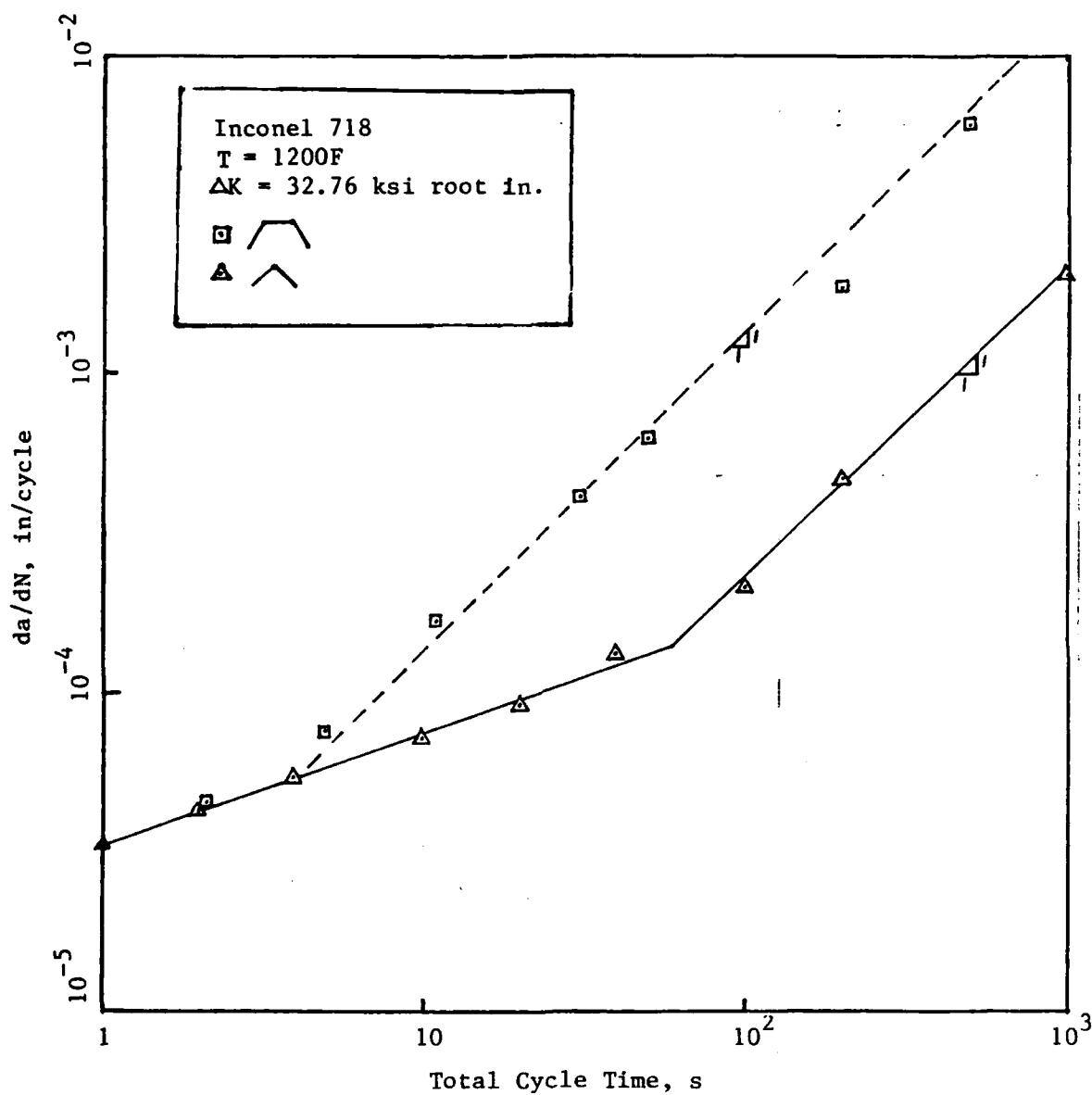
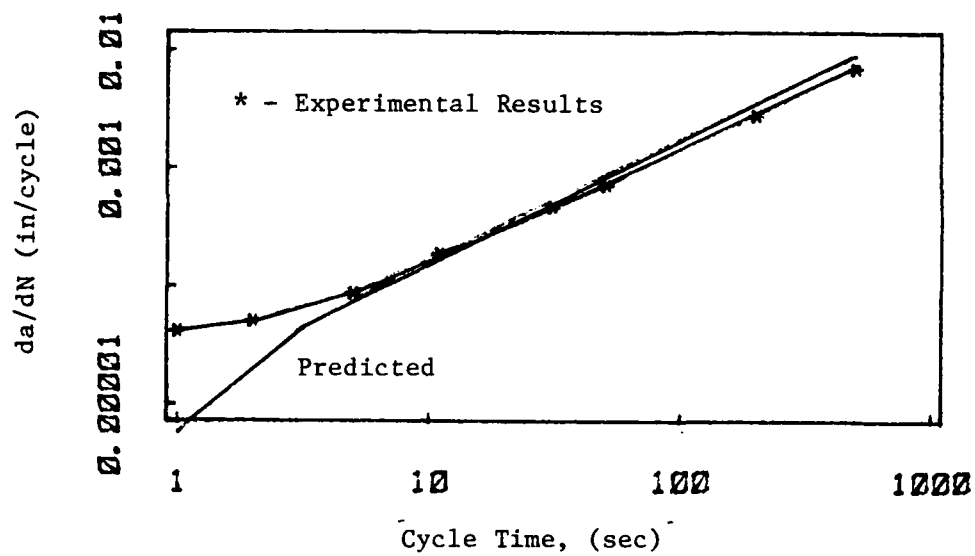
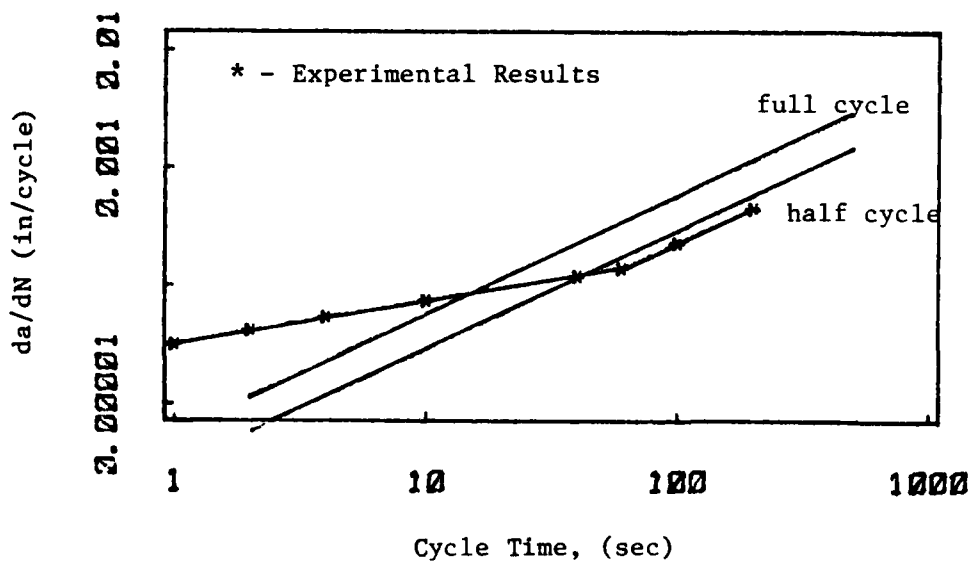


Figure 18. Fatigue-Creep Crack Growth Rate  $da/dN$ , for the two wave-forms shown.



a. Hold-time variation.



b. Frequency variation.

Figure 19. Comparison plots of Inconel 718 for  $R=.1$ ,  $T = 1200$  F, and  $\Delta K = 32.76$  ksi root in.

## V. Conclusions and Recommendations

Based on the analytical and experimental results, the following conclusions can be made for the evaluation of fatigue-creep crack growth of an engine alloy and the models used to analyze their behavior.

### SINH

The SINH model is a flexible program that can be used to accurately predict crack growth rates for more than one material. All or part of the model's curve can be used by properly selecting the equation's constants,  $C_2$  through  $C_4$ . Since the SINH curve does not have asymptotes, this equation behaves well for extrapolating to stress intensity ranges ( $\Delta K$ ) outside of those given in the experimental data.

As shown in Figure 14, SINH's description of crack growth variation with increasing hold-times was nonlinear on logarithmic coordinates. This nonlinearity was believed to be caused by the response of AF115 to the change in hold-time. For instance, in Figure 12, there was a smaller shift between the 90 and 300 second data sets than between the 0 and 90 second data sets. This weak dependency on hold-time at the longer duration cycletime shows up in Figure 14 as a nonlinearity for cycle times greater than 90 seconds. At a load of 22.77 ksi in  $1/2$ . For hold-time variation, the SINH model assumes that the constants  $C_2$ - $C_4$  in Eq (4) vary according to Eq (5), where FNCTN is equal to  $-\log(t_H)$ . The

method of determining the interpolative constants  $a$  through  $f$  in Eq (5) is described in Appendix C. If the experimental data, used to determine  $a$  through  $f$ , does not correlate with this assumed model then the model will produce nonlinear results, as shown in Figure 14. Since there is a weak dependency on hold-time for hold-times greater than 90 seconds (Figure 12), the SINH model produced nonlinear results in Figure 14 for cycle times greater than 90 seconds. Had the experimental data correlated with the assumed model in SINH, the results of Figure 14 should be similar to Figure 15. Notice that in Figure 14 at a  $\Delta K$  of 32.76 ksi (in)<sup>1/2</sup> that the result is more linear. Referring to Figure 12, there was a wider shift between the 90 and 300 second data sets at a  $\Delta K$  of 33 ksi (in)<sup>1/2</sup>. This confirms that as the dependency on hold-time strengthens the SINH model will produce more linear behavior.

All data, in Figure 18, can be fitted to a single SINH curve. Therefore, the crack growth rate ( $da/dN$ ) do not vary with frequency. An interpolative model for frequency was developed from the SINH model to examine SINH's description of crack growth rate with changing frequency. This interpolative model should produce no variation of crack growth rates with changing frequency. But as seen in Figure 16 this was not the case. In Figure 18, the inflection points (indicated by the solid squares) for each of the three SINH curves shift up and to the right as the frequency decreases. The three data groups that these curves were fitted to also

shift in the same direction. Because of this shift in the experimental data, the SINH model does not produce the same equation for the three data groups. Hence Figure 16 is not independent of frequency. The same argument can be made for the nonlinearity in Figure 16 as was made for Figure 14 in the previous paragraph.

### MSE

The MSE model only requires the four test parameters (stress ratio, temperature, frequency, and hold-time) to arrive at the associated crack growth rate equation. Again, this model is only applicable to AF115 material. This model has the ability to fit experimental data which is nonsymmetric. In other words, the model is not required to be symmetric about its inflection point. Models regarding the interpretation of crack growth rates with hold-time or frequency variation were incorporated into the MSE model. These models were intended to be linear in logarithmic coordinates (see Figures 13 and 15).

### SINH-MSE Comparison

The examination of the SINH and the MSE models' ability to predict crack growth rates has led to the following conclusions. First, both models lose accuracy as hold-time increases. Second, the number of cycles to failure decrease with increasing hold-times. Lastly, on the average the SINH model produced more accurate P/A values than the MSE model for the data analyzed (see Table 3).

### Predictive Model

The validity of Eq (19) was strictly within the creep dominant range of the experimental data used for comparison. This model produced accurate predictions when the frequency was greater than 5 seconds or the frequency was less than .02 Hertz. Therefore, this model should only be implemented within these regions when investigating the crack growth rate behavior of Inconel 718. From Figure 19, even for very low frequencies ( $< .002$  Hz), most of the damage accrued during cycling occurs only over 50% of the wave-form. This portion of the wave-form, over which damage occurs, may be the loading portion, unloading portion, or a mixture of both.

### Recommendations

A sufficient body of AF115 data should be collected in order to produce a graph similar to the one shown in Figure 18. This new information on AF115 can be used to determine if either SINH's or MSE's interpretation of crack growth rate with cycle time is correct for the data analyzed.

As flexible as the SINH model is, engineering judgement must be called upon when analyzing data. Seldom will the model produce the best possible results on the first attempt. One must examine the data beforehand to determine the appropriate input parameters required to arrive at the optimum output. The procedure used to arrive at this best fit to a set of data is more likely to be iterative, where

previous tries are revised in hopes of obtaining better curve fits to experimental data. The SINH model is a sophisticated curve fitting and data regression program that is specialized for cyclic crack growth rate data. More than a few weeks are required to fully understand all aspects of this model.

Enhanced understanding of fatigue-creep processes would be achieved if an empirical or analytical model could be developed to explain the crack growth behavior at cycle times less than 50 seconds for the experimental data given in Figure 19b. This region consists of mixed forms of fatigue and creep crack growth processes.

## Appendix A

The hyperbolic sine is defined as

$$y = \sinh x = (\exp(x) - \exp(-x))/2 \quad (\text{A.1})$$

and when presented in cartesian coordinates it appears as shown in Figure 20. The function is zero at  $x=0$  and has its inflection there.

The introduction of the four regression coefficients  $C_1$  through  $C_4$  permits relocation of the point of inflection and scaling of both axes. In the equation

$$(y-C_4) = \text{SINH } (x+C_3) \quad (\text{A.2})$$

$C_3$  establishes the horizontal location of the hyperbolic sine point of inflection, and  $C_4$  locates its vertical position.

To scale the axes,  $C_1$  and  $C_2$  are introduced

$$(y-C_4)/C_1 = \sinh (C_2(x+C_3)) \quad (\text{A.3})$$

which can be written as

$$y = C_1 \sinh (C_2(x+C_3)) + C_4 \quad (\text{A.4})$$

of which Eq (4) is a special case where  $y = \log (da/dN)$  and  $x = \log (\Delta K)$ . Note that  $C_1$  and  $C_2$  are dimensionless and can be thought of as stretching the curve vertically and horizontally respectively. Test results have shown that,

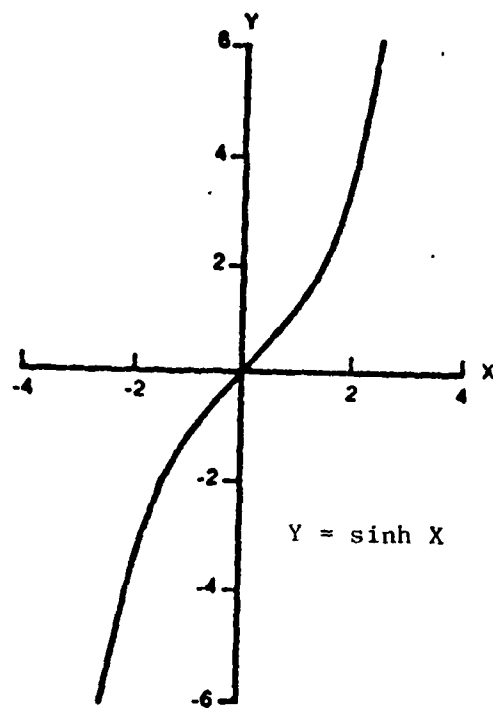


Figure 20. Hyperbolic Sine Function.

for a given material,  $C_1$  can be fixed without adversely affecting model flexibility (7:36-100).

Interpolative modeling of crack propagation as a function of operating parameters such as holdtime, frequency, stress ratio, and temperature requires a multiple regression capability which allows simultaneous consideration of several different data sets, each differing from the others by only one operating parameter. The model is to have broad interpolative capability with behavior at one condition used to describe crack propagation at another condition, since all possible stress conditions can not be tested in the laboratory.

Pratt and Whitney Aircraft has developed a mathematical technique to accomplish this. Individual sets of data are treated independently relative to some of the SINH coefficients, while the entire collection is treated as an entity with respect to the interpolative coefficients ( $C_{33}$ - $C_{38}$  discussed later).

The method of least squares is the computational procedure employed in the modeling of Eq (A.4) to the data. The goal of this procedure is to determine model coefficients for which the resulting curve through the data will have the minimum summed squared error between calculated and observed values for the dependent variable (see Figure (21)). In this instance, the independent and dependent variables are  $\log (\Delta K)$  and  $\log (da/dN)$ , respectively.

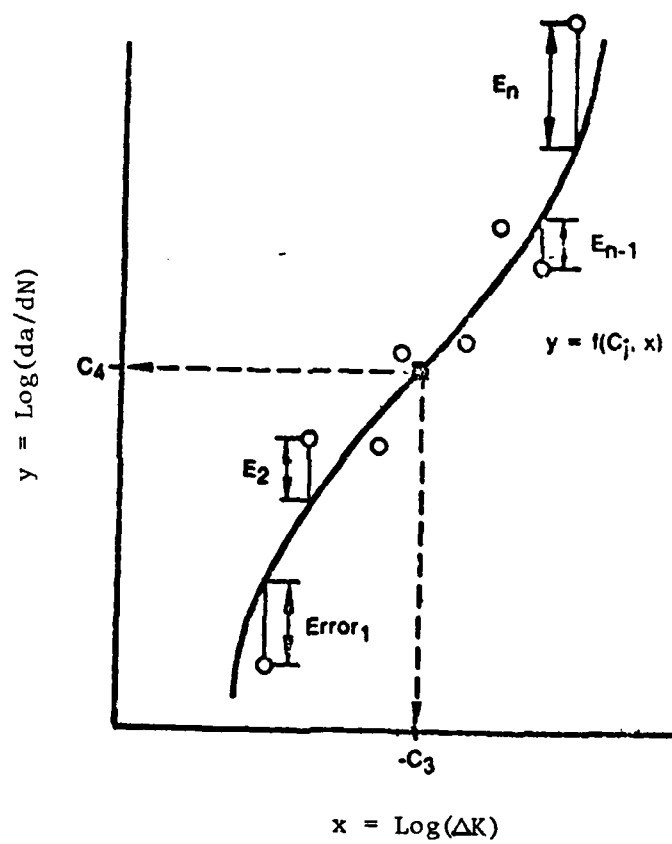


Figure 21. Error Determination between Observed and Calculated Data.

The sum of the squared errors is defined as

$$E^2 = \sum_{i=1}^N E_i^2 = \sum_{i=1}^N (Y_{CALi} - Y_i)^2 \quad (A.5)$$

where  $N$  is the number of data points.

Since  $Y_{CALi} = f(C_2, C_3, C_4, X_i)$  from Eqs (A.4),  $E$  is also a function of  $C_2$ ,  $C_3$ , and  $C_4$ .

Now,  $E^2$  will be a minimum when each of its partial derivatives is zero simultaneously. That is

$$\frac{\partial E^2}{\partial C_2} = \frac{2E \partial E}{\partial C_2} = 0 \quad (A.6)$$

$$\frac{\partial E^2}{\partial C_3} = \frac{2E \partial E}{\partial C_3} = 0 \quad (A.7)$$

$$\frac{\partial E^2}{\partial C_4} = \frac{2E \partial E}{\partial C_4} = 0 \quad (A.8)$$

when  $f$  is the SINH model,

$$E_i = C_1 \sinh (C_2(X_i + C_3)) + C_4 - Y_i \quad (A.9)$$

and

$$\frac{\partial E}{\partial C_2} = C_1 \cosh (C_2(X_i + C_3))(X_i + C_3) \quad (A.10)$$

$$\frac{\partial E}{\partial C_3} = C_1 \cosh (C_2(X_i + C_3))(C_2) \quad (A.11)$$

$$\frac{\partial E}{\partial C_4} = 1 \quad (A.12)$$

Now, substituting Eqs (A.9) - (A.12) into Eqs (A.6), (A.7), and (A.8), and solving the resulting three simultaneous equations provides values for  $C_2$ ,  $C_3$ , and  $C_4$  for which Eq (A.5) will be a minimum. In this instance, the resulting simultaneous equations are nonlinear in  $C_2$ ,  $C_3$ , and  $C_4$ . The solution, therefore, requires an iterative procedure. The user inputs the initial guesses for the constants and iteration then continues until the sum of the partial derivatives (Eqs (A.6), (A.7), and (A.8)), is less than  $10^{-6}$  or until the program reaches a maximum user specified iteration count. The maximum possible iteration count and the minimum required partial derivative sum are permanently set at 150 and  $10^{-6}$  respectively.

The foregoing discussion explains the procedure for determining the coefficients for a SINH curve corresponding to a particular set of data. Suppose further that each SINH representation of fatigue crack propagation is related to other SINH curves, the relationship depending on the differences in a test parameter between each data set. Consider hold-time as the changing test parameter between each data set as an example, and assume that the points of inflection are linearly related, namely

$$C_{3,j} = C_{33} + C_{34}(C_{4,j}) \quad (A.13)$$

for  $j$  different SINH curves which are fitted to  $j$  different data sets. The only changing parameter between each set is the hold-time.

Assume also that  $C_2$  and  $C_4$  are related to hold-time by Eqs (A.14) and (A.15).

$$C_{4,j} = C_{35} + C_{36}(-\log(t_H)) \quad (A.14)$$

$$C_{2,j} = C_{37} + C_{38}(-\log(t_H)) \quad (A.15)$$

The functional relationships  $(-\log(t_H))$  are defined in Table 1. Coefficients  $C_{33}$  through  $C_{38}$  can be then determined by substituting Eqs (A.13), (A.14), and (A.15) into Eq (A.9) and differentiating with respect to  $C_{33}$  through  $C_{38}$  in a manner analogous to that used in determining  $C_2$ ,  $C_3$ , and  $C_4$  in the foregoing discussion. The constants  $a$  through  $f$  in Eqs (5) are the appropriate constants  $C_{33}$  through  $C_{38}$  of Eqs (A.13), (A.14), and (A.15). For complete development of the SINH model see (7). For explicit use of the program and its listing refer to (16).

## APPENDIX B

This section presents the computer code listing of General Electric's model. This listing is a revised version of the one presented in (6). The program is written in a Fortran computer language and operates from the Vax 11/780 computer hardware system located at the Air Force Institute of Technology, Wright-Patterson AFB, OH. This program is interactive and will prompt the user for the desired test parameters. After calculation of the six coefficients, the program will ask the user if values of crack growth rates are desired. If so, the program will prompt the user for the required information.

```

program ge mod
real n1,n2,mm
real mrpt9,n
open(2,file='calge2y',status='new')
open(3,file='calge2x',status='new')
1100 print *, 'Input Temperature (degrees F):'
read *,t
print *, 'Input Stress Ratio:'
read *,r
print *, 'Input Inverse Freq. (sec/cyc):'
read *,tc
print *, 'Input Hold Time (sec.):'
read *,ht
v025=0.025-1.e-20
t999=1000.-1.e-10
tpt4=.4-1.e-10
rpt9=.9+1.e-10
s=-5.3+4.4e-3*t
if(s.lt.1.0)s=0.0
n=8.e-04*t-0.04
if(n.lt.1.0)n=1.0
b=(t-1200)*.0018-4.52
if(r.gt..5)xcons=.69897
if(r.le..5)xcons2=.5
if(r.le..5)xcons=.25527
if(r.gt..5)xcons2=.1
if(b.gt.-4.52)b=-4.52
y1=s*(alog10(tc/tpt4))**n+b
n1=1.+1.16e-02*(t-t999)-2.81e-05*(t-t999)**2
s1=4.27e-13*(t-t999)**4.768+.2
b1=7.607e-13*(1400.-t)**4.605+4.77
b1=-b1
y2=b1*(alog10(tc/tpt4))**n1+b1
s2=2.145e-04*(t-t999)**1.444+.5
b2=-2.628e-03*(t-t999)**1.051+6.201
n2=.9855+1.096e-03*(t-t999)-4.366e-06*(t-t999)**2

```

```

b2=-b2
y3=s2*(alog10(tc/tpt4))**n2+b2
slope=(y1-y2)/.25527
c=y1-slope*(alog10(rpt9)-alog10(1-r))
slope2=(y2-y3)/.69897
if(r.le..5) go to 10
if(slope.lt.0.and.slope2.lt.0.and.slope2.gt.slope.or.slope.gt.0.
&and.slope2.gt.0.and.slope2.lt.slope)
&c=y2-slope2*(alog10(.5)-alog10(1-r))
10 continue
dadn=10.**c
v=1/tc
if(ht.eq.0.)go to 590
efct=0.
if(r.gt..5) go to 530
if(t.le.1200.)htb=0.0065*(t-1000)
efct=4.75e-03*((alog10(v/v025))**.9379-1.)
if(t.ge.1200)efct=efct*(t-1200)
if(t.le.1200)efct=0.
if(t.le.1200)hta=0.005*(t-1000.)
if(t.gt.1200)hta=1.
if(t.gt.1200)htb=5.75e-04*(t-1200)+1.3
htb=htb+efct
htq=htb+hta*(alog10(ht/20))
if(htq.lt.0.)htq=0.
dadn1=10.**(htq+(alog10(dadn)))
dadna=dadn1
530 continue
etb=1.456e-06*(t-1000.)**2.275*((alog10(v/v025))**(9.15e-04
&*(t-1000.)+.652)-1.)
br5=3.809e-02*(t-1000.)**.5905+etb
evt=(.55-1.739e-06*(t-1000.)**1.998)*((alog10(v/v025))**.25-1.)
cr5=.55+7.1578e-03*(t-1000.)-1.55e-05*(t-1000.)**2.+evt
htq5=br5+cr5*(alog10(ht/20.))
if(htq5.lt.0)htq5=0.
dadn5=10.**(htq5+(alog10(dadn)))
if(r.le..5)dadnb=dadn5
if(r.gt..5)dadna=dadn5
if(r.le..5) go to 535
evt9=.0.64-3.167e-05*(t-1000.)**1.513*((alog10(v/v025))**.32-1.)
c259=.64+6.572e-03*(t-1000.)-1.48e-05*(t-1000.)**2.
cr9=c259+evt9
br9=.15+.3543*(t-1000.)**.1339
xz=(.13+4.9e-05*(t-1000.)**1.56)*((alog10(v/v025))**1.8-1.)
br9=br9+xz
if(cr9.lt.0)cr9=0.
htq9=br9+cr9*(alog10(ht/20.))
if(htq9.lt.0)htq9=0.
dadn9=10.**(htq9+(alog10(dadn)))
dadnb=dadn9
535 dadn=(alog10(dadnb)+(alog10(dadna/dadnb))/xcons)*(alog10((1-r)
&/xcons2)))
dadn=10.**dadn
590 d1=1.25618-2.838e-09*(t-t999)**3.10561
d2=1.37103-5.03102e-10*(t-t999)**3.30553
a=2.081-(d1*(alog10(rpt9/(1-r))))**d2)
mm=.13
if(r.le.0.5)go to 17
mrpt=9.898e-06*(t-t999)**1.5847
slpm=(.13-mrpt9)/.69897
mm=.13-slpm*(alog10(.5/(1-r)))
17 continue
delk=10.**a*dadn**mm
xkc=122*(1-r)
xks=10.**(1.-((.232+8.406e-03*(t-1000)**.729)*(alog10(.9/(1-r)))))
if(delk.gt.xkc)delk=xkc-.0001
vht=1/(v+ht)
if(r.gt..5)go to 600
ttemp=t
if(t.gt.1300)ttemp=1300
e=1.55e-02*(ttemp-1200)*((alog10(v/v025))**.0902-1)
if(e.lt.0.)e=0.
prim=2.7+6.88e-03*(t-1000)-1.94e-05*(t-1000)**2.+e
if(ht.eq.0.)go to 599

```

```

a25t=2.737e-07*(ttemp-1000)**2.74
avt=a25t+e
bvt=5.346e-03*(ttemp-1000)**.7331
qvtht=avt+bvt*(alog10(ht/20.))
prim=prim-qvtht
if(t.le.1200)up=2.7-1.e-03*(t-1000)
if(t.gt.1200)up=2.6-.1372*(t-1200)**.5194
if(prim.lt.up)prim=up
599 prima=prim
600 continue
gama=1.7-8.25e-10*(t-1000)**3.54
e=1.734e-10*(t-1000)**3.807*((alog10(v/v025))**gama-1)
prim=2.25+6.875e-03*(t-1000)-2.188e-05*(t-1000)**2.+e
if(ht.eq.0)go to 610
a25t=1.652e-02*(t-1000)**.6616
alpha=.5220+4.23e-03*(1400-t)
if(alpha.gt.1.37)alpha=1.37
beta=.152+7.165e-03*(1400-t)
if(beta.gt.1.59)beta=1.59
b25t=.1300*(t-1000)**.111
avt=a25t+3.18e-03*(t-1000)**2.86*((alog10(v/v025))**alpha-1)
bvt=b25t+4.50e-11*(t-1000)**3.755*((alog10(v/v025))**beta-1)
qvtht=avt+bvt*(alog10(ht/20.))
prim=prim-qvtht
up=2.25-2.613e-09*(t-1000)**3.426
610 if(prim.lt.up)prim=up
if(r.le..5)primb=prim
if(r.gt..5)prima=prim
if(r.le..5)go to 620
e=4.351e-03*(t-1000)**.7225*((alog10(v/v025))**1.34-1)
prim=1.4+5.425e-03*(t-1000)-1.963e-05*(t-1000)**2.+e
if(ht.eq.0)go to 619
alpha=1.705+2.66e-03*(1400-t)
a25t=7.87e-06*(t-1000)**1.716
if(alpha.gt.2.237)alpha=2.237
avt=a25t+7.871e-06*(t-1000)**1.716*((alog10(v/v025))**alpha-1)
b25t=1.575e-03*(t-1000)-2.875e-06*(t-1000)**2.
gama=.8194-2.49e-03*(1400-t)
if(gama.lt.0.322)gama=.322
evt=b25t*((alog10(v/v025))**gama-1)
bvt=b25t+evt
qvtht=avt+bvt*(alog10(ht/20.))
prim=prim-qvtht
up=1.5-7.e-03*(t-1200)
if(t.lt.1200)up=1.4+1.e-04*(t-1000)
if(prim.lt.up)prim=up
619 primb=prim
620 continue
prim=(alog10(primb)+((alog10(prima/primb))/xcons)*(alog10((1-r)
&/xcons2)))
dadnp=10.**prim
ape=alog10(2.5)+2.41e-03*(t-1000)
q=10.**(ape+.57*(alog10(.1/r)))
if(q.gt.3.)q=3.
srd=(sqrt(q)*(alog(xkc)-alog(delk)))/(alog(delk)-alog(xks))
d=-srd**2.
p=dadnp-(q/(alog(delk)-alog(xks)))+(d/(alog(xkc)-alog(delk)))
bp=alog(dadn)-q*alog(alog(delk)-alog(xks))-d*alog(alog(xkc)
c=alog(delk))
b=bp-p*(alog(delk)-alog(xks))
print 40,b,p,q,d,xks,xkc,dadn,dadnp
print 41,t,r,v,ht
40 format(6(2x,f8.4),e14.5,2x,f8.4)
41 format(4(f10.4,2x))
print *, 'Desire da/dn values? 1 for yes, 0 for no'
read *,flag1
if(flag1.eq.0) go to 999
1000 print *, 'Input desired delta K (ksi root in)'.
read *,dk
dadno=exp(b)*((dk/xks)**p)*((alog(dk/xks))**q)*
&((alog(xkc/dk))**d)

```

```

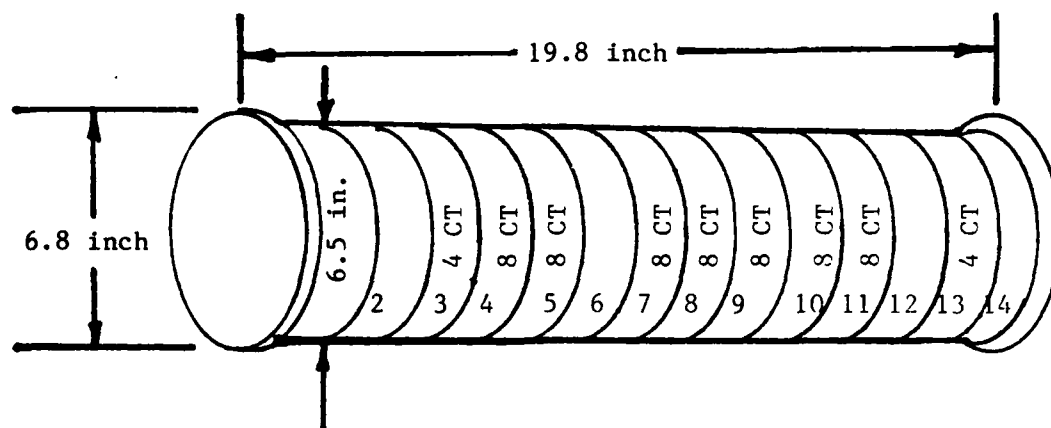
      print 42,dadno,dk
42 format(1x,'crack growth rate in in/cyc is:',e12.5,3x,
&'for dk=',f6.2,/)
      write(2,1)dadno
      1 format(e12.5)
      write(3,2)dk
      2 format(f6.2)
      Print *, 'Another da/dn value? 1 for yes, 0 for no'
      read *,flag2
      if(flag2.eq.1)go to 1000
999 print *, 'Change in test variables? 1 for yes, 0 for no'
      read *,flag3
      if(flag3.eq.1) go to 1100
      stop
      end

```

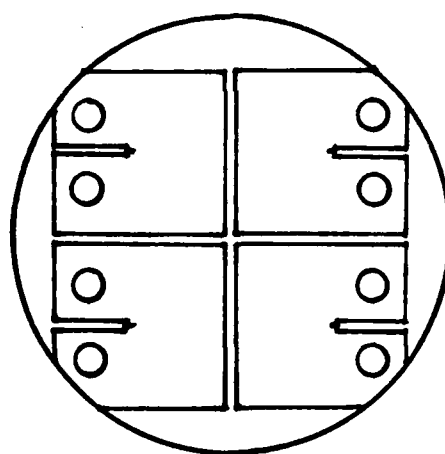
### Appendix C

AF115 is a gamma-prime strengthened nickel-base alloy in which titanium, aluminum, columbium, and hafnium are gamma prime formers and chromium, cobalt, molybdenum, and tungsten are strengtheners of the gamma matrix. The AF115 powder was produced by vacuum melting from virgin material and argon spray atomized to powder. Results of the chemical analysis conducted by the General Electric Company (6:2) of the powder are shown in Table 4.

This composition was produced by Carpenter Technology (6:7). They produced a cylindrical log with the dimensions shown in Figure 22a along with the location of the 14 slices used to produce test specimens. Figure 22b illustrates how the compact tension specimens were machined from each slice. Seven of the slices (1, 2, 3, 6, 12, 13, and 14) were used for density characterization, stress qualification, and thickness evaluation (6:3-14). The remainder of the slices each produced 8 compact tension specimens which were used for cyclic testing. The configuration of the machined compact tension specimens is illustrated in Figure 23. Because of the undersize diameter of the log, these specimens contained one beveled corner. It was located near one of the loading holes and had no influence on crack growth results (6:6).



a. Location of Slices from AF115 Material.



b. Orientation of 0.5 inch compact tension specimen machined from slices.

Figure 22. Location and Orientation of Compact Tension Specimens.

Table 4. Composition of AF115 Powder

| Element    | Percentage by Weight |
|------------|----------------------|
| Carbon     | 0.043                |
| Manganese  | 0.010                |
| Silicon    | 0.040                |
| Sulfur     | 0.002                |
| Chromium   | 10.680               |
| Titanium   | 3.850                |
| Aluminum   | 3.670                |
| Boron      | 0.019                |
| Zirconium  | 0.057                |
| Iron       | 0.130                |
| Cobalt     | 15.100               |
| Molybdenum | 2.800                |
| Tungsten   | 5.670                |
| Phosphorus | 0.005                |
| Hafnium    | 0.840                |
| Columbium  | 1.710                |
| Nickel     | Balance              |

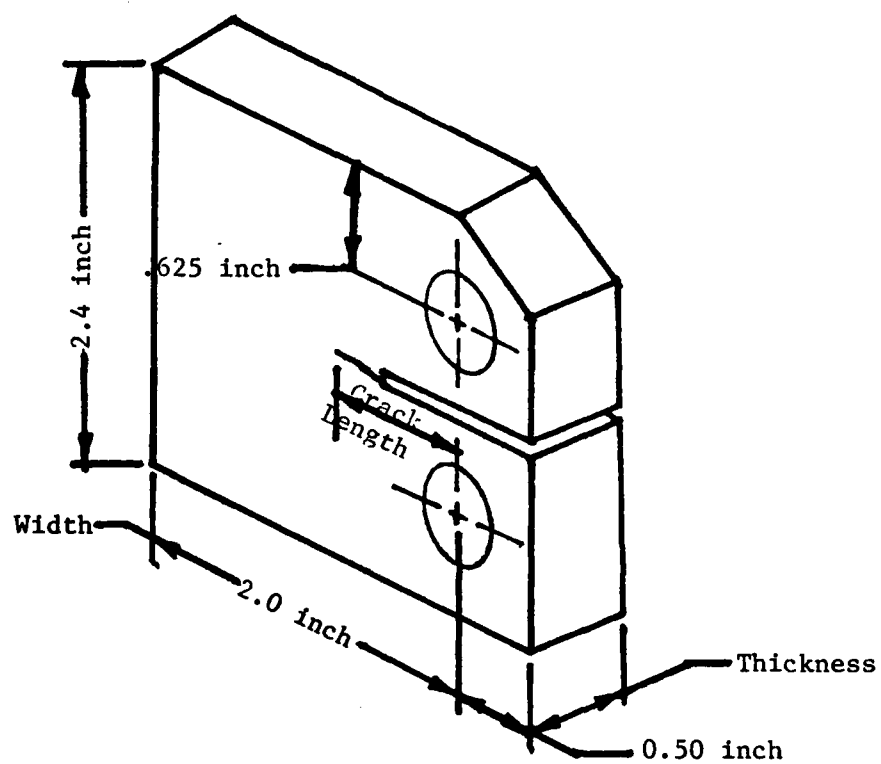


Figure 23. Configuration of Compact Tension Specimen.

The compact tension specimens were precracked at either room or elevated temperature. Initially, the specimens were precracked at room temperature at 30Hz with cyclic loads being stepped down in 10% increments as a function of precracked length. The final precrack length and applied loads produced a stress intensity range ( $\Delta K$ ) less than or equal to the initial stress intensity of the subsequent elevated temperature cyclic crack growth tests. About half of the specimens were precracked in this fashion. During the early stage of testing it appeared that the precracking was interfering with the normal crack growth behavior. The curvature of the crack would rapidly change shortly after initiation of testing. Because of this effect, precracking was conducted at elevated temperatures within the system used for testing so that the final precracking was done at the test conditions loads. Even then a few of the specimens produced uneven crack fronts (6:18).

Specimen heating was provided by a specially designed split shell three zone resistance furnace equipped with quartz viewing windows. Conventional 20X traveling microscopes were used to monitor crack growth on both surfaces of the specimens.

At the conclusion of each test, the raw crack length versus accumulative cycle data were reduced to cyclic crack growth rate ( $da/dN$ ) by use of the seven-point sliding polynomial technique recommended by the American Society for Testing and Materials (ASTM) (17). The cracks lengths were

adjusted for curvature by the ASTM recommended quarter width average crack length and maximum crack length technique (18). The stress intensity range value associated with the mid-crack length of each set of consecutive seven points was determined by:

$$\Delta K = \frac{\Delta P}{B(W)^{1/2}} \frac{2 + a/W}{(1-a/W)^{3/2}} (0.866 + 4.64(a/W) - 13.32(a/W)^2 - 5.62(a/W)^3) \quad (C.1)$$

where

$\Delta P$  = change in load ( $P_{max} - P_{min}$ )

$B$  = specimen thickness

$W$  = specimen width

$a$  = average crack length.

Thus pairs of  $da/dN$  and  $\Delta K$  values were available for model evaluation.

### Bibliography

1. Burke, John J. and Volker Weiss. Fatigue Environment and Temperature Effects. New York: Plenum Press, 1983.
2. "Analysis of Life Prediction Methods for Time-Dependent Fatigue Crack Initiation in Nickel-Base Super Alloys", National Materials Advisory Board, Publication NMAB-347, National Academy of Sciences, Washington, DC, 1980.
3. Cruse, T.A. and Meyer, T.G., "Structural Life Prediction and Analysis Technology", Air Force Aero Propulsion Laboratory Report AFAPL-TR-78-106, Wright-Patterson AFB, OH, 1978.
4. Hill, R.J., Reimann, W.H., and Ogg, S.S., "A Retirement-for-Cause Study of an Engine Turbine Disk", Unpublished Air Force Wright Aeronautical Laboratories Report.
5. Harris, J.A., Jr, Sims, D.L., and Annis, C.B., Jr, "Concept Definition: Retirement for Cause of F100 Rotor Components", Air Force Wright Aeronautical Laboratories Report, AFWAL-TR-80-4118, Wright-Patterson AFB, OH, 1980.
6. Utah, David A..Crack Growth Modeling in and Advanced Powder Metallurgy Alloy, 1 Sept 1977--1 Feb 1980. Contract AFWAL-TR-80-4098. Air Force Wright Aeronautical Laboratories, Wright-Patterson Air Force Base, OH, July 1980.
7. Larsen J.M., Schwartz B.J., and Annis C.G., Jr.. Cumulative Damage Fracture Mechanics Under Engine Spectra, Sept 1977--Jan 1980. Contract AFML-TR-79-4159. Air Force Wright Aeronautical Laboratories, Wright-Patterson Air Force Base, OH, Jan 1980.
8. Shahinian P. and Sadananda K.. "Effects of Stress Ratio and Hold-Time on Fatigue Crack Growth in Alloy 718," Journal of Engineering Materials and Technology, Vol. 101: 224-230 (July 1979).
9. Bartos, J.L. Development of a Very High Strength Disk Alloy for 1400F Service, Contract AFML-TR-74-187, General Electric Company, Dec, 1974.

10. International Mathematical and Statistical Libraries, Inc. IMSL Library. Reference Manual. Houston, TX: IMSL, Inc., July, 1980.
11. Nicholas T., Weenasooriya T., and Ashbaugh N.E.. "A Model for Creep/Fatigue Interaction in Alloy 718," ASTM Sixteenth National Symposium on Fracture Mechanics, Battelle Columbus Laboratory, Columbus OH, 15-17 Aug. 1983.
12. Ashbaugh N.E.. "Creep Crack Growth Behavior in IN718," ASTM Sixteenth National Symposium On Fracture Mechanics, Battelle Columbus Laboratory, Columbus OH, 15-17 Aug, 1983.
13. Larsen, J.L., and Annis, GG. "Cumulative Damage Fracture Mechanics Under Engine Spectrum," Annual Report on Air Force Material Laboratory Contract F33615-77-C-5153, Pratt and Whitney Aircraft/Government Products Division, September 1978.
14. Wheeler, O.E., "Spectrum Loading and Crack Growth," Journal of Basic Engineering, American Society for Mechanical Engineering, 1972, pp. 181-186.
15. Willenborg, J., Engle, R.M., and Wood, H.A., "A Crack Growth Retardation Model Using an Effective Stress Concept," AFFDL-TM-71-1-FRR, Air Force Flight Dynamics Lab, 1971.
16. Schwartz, B.S., Larsen, J.M., Annis, C.G., "Cumulative Damage Fracture Mechanics Under Engine Spectra: Fortran User's Manual for Super SINH," Prepared for Air Force Materials Laboratory Contract F33615-77-C-5153, Pratt and Whitney Aircraft/Government Products Division, January 1980.
17. Annual Book of ASTM Standards, Part 10 E467.
18. Annual Book of ASTM Standards, Part 10 E399.

### Vita

Jeffery Roy Christoff was born on 9 November 1959 in Mobile, Alabama. He graduated from High School in Boerne, Texas in 1978 and attended Texas A&M University, College Station, Texas, from which he received the Degree of Bachelor of Science in Aerospace Engineering in May 1982. He entered the Air Force on active duty in May 1982, and received his commission from Reserve Officer Training Corps in May 1982. He entered the School of Engineering, Air Force Institute of Technology, in June 1982. He is a member of Tau Beta Pi and Sigma Gamma Tau.

Permanent Address: 103 Cedar St.  
Boerne, TX 78006

Unclassified

SECURITY CLASSIFICATION OF THIS PAGE

REPORT DOCUMENTATION PAGE

|   |       |  |  |   |          |
|---|-------|--|--|---|----------|
| 1a. REPORT SECURITY CLASSIFICATION<br>Unclassified  |       |  | 1b. RESTRICTIVE MARKINGS   |   |          |
| 2a. SECURITY CLASSIFICATION AUTHORITY   |       |  | 3. DISTRIBUTION/AVAILABILITY OF REPORT<br>Approved for public release;<br>distribution unlimited |   |          |
| 2b. DECLASSIFICATION/DOWNGRADING SCHEDULE   |       |  |  |   |          |
| 4. PERFORMING ORGANIZATION REPORT NUMBER(S)<br>AFIT/GA/AA/83D-2   |       |  | 5. MONITORING ORGANIZATION REPORT NUMBER(S)  |   |          |
| 6a. NAME OF PERFORMING ORGANIZATION<br>School of Engineering<br>Air Force Inst. of Tech.  |       | 6b. OFFICE SYMBOL<br>(If applicable)<br>AFIT/EN              | 7a. NAME OF MONITORING ORGANIZATION  |   |          |
| 6c. ADDRESS (City, State and ZIP Code)<br>Air Force Institute of Technology<br>Wright-Patterson AFB, OH, 045433   |       |  | 7b. ADDRESS (City, State and ZIP Code)   |   |          |
| 8a. NAME OF FUNDING/SPONSORING ORGANIZATION   |       | 8b. OFFICE SYMBOL<br>(If applicable)                         | 9. PROCUREMENT INSTRUMENT IDENTIFICATION NUMBER  |   |          |
| 8c. ADDRESS (City, State and ZIP Code)  |       |  | 10. SOURCE OF FUNDING NOS.   |   |          |
|   |       |  | PROGRAM ELEMENT NO.  | PROJECT NO.   | TASK NO. |
| 11. TITLE (Include Security Classification)<br>See Box 19   |       |  |  |   |          |
| 12. PERSONAL AUTHOR(S)<br>Jeffery R. Christoff, Second Lieutenant, USAF   |       |  |  |   |          |
| 13a. TYPE OF REPORT<br>MS Thesis  |       | 13b. TIME COVERED<br>FROM _____ TO _____                     |  | 14. DATE OF REPORT (Yr., Mo., Day)<br>83 December 1 |          |
|   |       |  |  | 15. PAGE COUNT<br>71                                |          |
| 16. SUPPLEMENTARY NOTATION<br><div style="text-align: right;">Approved for public release: IAW AFR 190-17.<br/><i>[Signature]</i><br/>LYNN E. WOLVER<br/>Dean for Research and Professional Development<br/>Air Force Institute of Technology (AFIT)<br/>Wright-Patterson AFB, OH 45433</div> |       |  |  |   |          |
| 17. COSATI CODES  |       |  | 18. SUBJECT TERMS (Continue on reverse if necessary and identify by block number)                |   |          |
| FIELD   | GROUP | SUB. GR.   |  |   |          |
| 20  | 11    |  | Fatigue, creep, crack growth, high temperature fracture  |   |          |
| 19. ABSTRACT (Continue on reverse if necessary and identify by block number)  |       |  |  |   |          |
| Title: Evaluation of Fatigue-Creep Crack, Growth in an Engine Alloy   |       |  |  |   |          |
| Thesis Chairman: George Haritos, Major, USAF  |       |  |  |   |          |
| 20. DISTRIBUTION/AVAILABILITY OF ABSTRACT<br>UNCLASSIFIED/UNLIMITED <input checked="" type="checkbox"/> SAME AS RPT. <input type="checkbox"/> DTIC USERS <input type="checkbox"/>   |       |  | 21. ABSTRACT SECURITY CLASSIFICATION<br>Unclassified   |   |          |
| 22a. NAME OF RESPONSIBLE INDIVIDUAL<br>George K. Haritos, Major USAF  |       | 22b. TELEPHONE NUMBER<br>(Include Area Code)<br>513-255-2998 |  | 22c. OFFICE SYMBOL<br>AFIT/ENY                      |          |

This study investigates fatigue-creep interaction effects in alloys and evaluates the effectiveness of predictive models currently in use by the aircraft engine industry. The state-of-the-art crack growth rate prediction models are supplied by the General Electric Company (MSE) model, and the Pratt and Whitney Aircraft Group (SINH) model. They are used to predict crack rates under a range of conditions which involve fatigue-creep interactions.

Another aspect of this study involves the development of an empirical model to predict fatigue-creep crack growth based on creep crack growth rate data and knowledge of the loading waveform. This study is primarily directed toward high temperature ( $\leq 1000$  F) fatigue-creep interaction at low test frequencies and positive stress ratios.

The SINH model proves to be more accurate than the MSE model in predicting crack growth rates for the data analyzed. Both models predict linear relationships for the variation of crack growth rates ( $da/dN$ ) with the length of hold-time or the frequency rate on logarithmic coordinates. The MSE model is developed for AF115, whereas the SINH model has the ability to adapt to any high-strength material.

The predictive model, developed in this paper, compares well with experimental fatigue-creep crack growth rate data that are mostly in the time-dependent regime, that is, when hold-times are in excess of 5 seconds or the frequency is less than .02 cycles/second. This model correlates well with experimental data tested at these conditions.

**END**

**FILMED**

**2-84**

**DTIC**